



**HAL**  
open science

## A dynamic game approach to uninvadable strategies for biotrophic pathogens

Ivan Yegorov, Frédéric Grognard, Ludovic L. Mailleret, Fabien Halkett, Pierre Bernhard

► **To cite this version:**

Ivan Yegorov, Frédéric Grognard, Ludovic L. Mailleret, Fabien Halkett, Pierre Bernhard. A dynamic game approach to uninvadable strategies for biotrophic pathogens. *Dynamic Games and Applications*, 2020, 10, pp.257-296. 10.1007/s13235-019-00307-1 . hal-02147836

**HAL Id: hal-02147836**

**<https://inria.hal.science/hal-02147836v1>**

Submitted on 5 Jun 2019

**HAL** is a multi-disciplinary open access archive for the deposit and dissemination of scientific research documents, whether they are published or not. The documents may come from teaching and research institutions in France or abroad, or from public or private research centers.

L'archive ouverte pluridisciplinaire **HAL**, est destinée au dépôt et à la diffusion de documents scientifiques de niveau recherche, publiés ou non, émanant des établissements d'enseignement et de recherche français ou étrangers, des laboratoires publics ou privés.

## A dynamic game approach to uninvadable strategies for biotrophic pathogens

Ivan Yegorov · Frédéric Grogard ·  
Ludovic Mailleret · Fabien Halkett ·  
Pierre Bernhard

Received: / Accepted:

**Abstract** This paper studies a zero-sum state-feedback game for a system of nonlinear ordinary differential equations describing one-seasonal dynamics of two biotrophic fungal cohorts within a common host plant. From the perspective of Adaptive Dynamics, the cohorts can be interpreted as resident and mutant populations. The invasion functional takes the form of the difference between the two marginal fitness criteria and represents the cost in the definition of the value of the differential game. The presence of a specific competition term in both equations and marginal fitnesses substantially complicates the reduction of the game to a two-step problem that can be solved by using Optimal Control Theory. Therefore, a general game-theoretic formulation involving uninvadable strategies has to be considered. First, the related Cauchy problem for the Hamilton–Jacobi–Isaacs equation is investigated analytically by the method of characteristics. A number of important properties are rigorously derived. However, the complete theoretical analysis still remains an open challenging problem due to the high complexity of the differential game. That is why an ad hoc conjecture is additionally proposed. An informal but rather convincing and practical justification for the latter relies on numerical simulation results. We also establish some asymptotic properties and provide biological interpretations.

---

I. Yegorov (✉)  
North Dakota State University, USA  
E-mail: ivanyegorov@gmail.com  
Also known as I. Egorov

F. Grogard · P. Bernhard · L. Mailleret  
Université Côte d’Azur, Inria, INRA, CNRS, Sorbonne Université, Biocore team, France

L. Mailleret  
Université Côte d’Azur, INRA, CNRS, ISA, France

F. Halkett  
UMR IAM, INRA, Université de Lorraine, Nancy, France

**Keywords** Uninvadable strategy · Zero-sum differential game · Biotrophic pathogens · Resource allocation · State-feedback control · Hamilton–Jacobi–Isaacs equation · Method of characteristics · Finite-difference approximation

## 1 Introduction

In compliance with Darwin’s Theory of Evolution by Natural Selection, it is relevant to model the mechanisms by which various biological species allocate available resources with the objective either to maximize their fitness criteria or to prevent invasions of others [1]. The first type of strategies is usually governed by specific optimality principles for relatively isolated homogeneous populations and hence may not be reasonable in case of competition for common resources between different populations or between resident and mutant genotypes. For instance, the mutants may take evolutionary advantage by acting differently from the residents.

A number of mathematical techniques have been developed to study the strategies that can be selected through evolution among competing genotypes. Adaptive Dynamics is of particular interest there. This methodology is based upon the analysis of how resident populations allow or prevent invasions by rare mutants [2, 3]. The concept of evolutionary stable strategy (or, in short, ESS) originally introduced in the context of Evolutionary Game Theory [4, 5] plays a crucial role in Adaptive Dynamics. An ESS can informally be described as a point in the trait space at which no mutant population can invade. ESS-es therefore lead to evolutionary equilibria [3, §3.7]. Despite their name, ESS-es may nevertheless form (dynamically) unstable equilibria [6, 7].

Classical results of Adaptive Dynamics focused mainly on finite-dimensional traits. However, many actual dynamic life-history characteristics could have an infinite-dimensional nature, especially those subjected to dilemmas of resource allocation. Therefore, some recent developments in Adaptive Dynamics considered function-valued traits [8–12]. The following approach to compute ESS-es was proposed in [10, 11]: maximize the invasion fitness over admissible mutant strategies  $u_{\text{mut}}$  and thereby construct the set of maximizers  $U_{\text{mut}}^*(u_{\text{res}})$  depending on an admissible resident strategy  $u_{\text{res}}$ , then a solution  $\hat{u}_{\text{res}}$  to the inclusion  $u_{\text{res}} \in U_{\text{mut}}^*(u_{\text{res}})$  is an ESS if the corresponding invasion fitness maximizer is unique, i. e., if  $U_{\text{mut}}^*(\hat{u}_{\text{res}}) = \{\hat{u}_{\text{res}}\}$ . The latter uniqueness ensures that the related symmetric Nash equilibrium is strict and consequently represents an ESS (see [13, §2.1]). But efficient practical applications of this approach (including the usage of Pontryagin’s maximum principle from Optimal Control Theory [14]) were limited to models in which the resident dynamics and fitness did not explicitly depend on the mutant population. Otherwise, one has to use the general formulation of [11, §4.1] involving the concepts of uninvadable strategy and Wardrop equilibrium and leading to a zero-sum two-player differential game.

The aim of this work is to investigate a game-theoretic extension of the dynamic optimization problem of [15]. The latter was to find a resource allocation

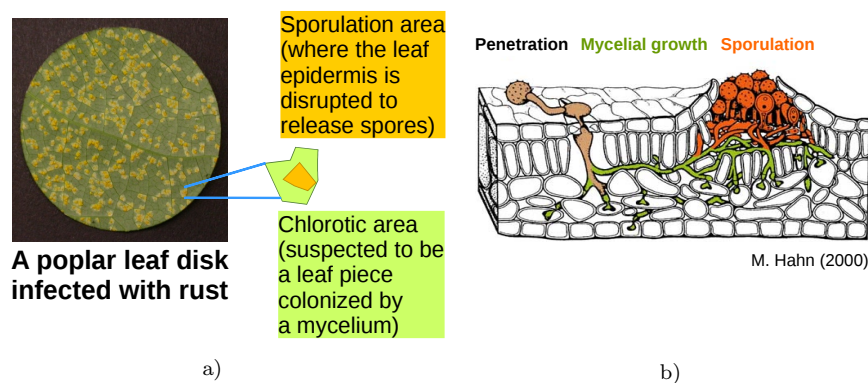


**Fig. 1** a) *Rust lesions scattered on a poplar leaf disk in a laboratory experiment. When zooming in on a lesion, one can distinguish an orange-yellow sporulation area (corresponding to the spores produced by the lesion) and a pale yellow-green chlorotic area (colonized by a mycelium). Note that chlorotic areas are not always clearly visible, depending on host genetic backgrounds.* b) *Schematic illustration of a rust infection cycle, as presented in [17]. The permission to use this illustration in the current paper was obtained from Springer Nature via an order through Copyright Clearance Center's RightsLink® service (the license number 4513210982653).*

strategy maximizing the pathogen fitness (analogous to the lifetime reproductive success) for one-seasonal development of a single biotrophic fungal cohort within one host plant.

Biotrophic fungi are an important group of plant pathogens [16, 17]. The mass of branching and thread-like hyphae constituting the vegetative part of such a fungus is called the mycelium. The fungi permeate living host plant cells and obtain nutrients from the latter via specific absorbing organs that appear as outgrowths of the somatic hyphae and are called haustoria. Thereby, the hosts are harmed but not killed. In natural environments, this kind of parasitism decreases competitive abilities of plants. It also reduces yields in agricultural systems. A significant subclass of biotrophic fungi contains rust fungi causing such diseases as leaf rusts of poplar, willow, wheat, blackberry, etc. Another subclass consists of powdery mildew fungi infecting such emblematic/cultivated species as oaks, grapes, hawthorn, gooseberry, etc., and, of course, many species of wild plants. The model of [15] considered a biotrophic fungal cohort allocating available host resources between two different activities, namely mycelial growth (within-host multiplication) and sporulation (production of spores for outer transmission of the infection). Some related illustrations are given in Fig. 1.

In [15], the constructed feedback form of the optimal allocation strategy indicated a key role of a singular regime with coexisting activities (after the onset of sporulation). This is common among biotrophic fungi (see, e. g., [18–20] and note that, if the average mycelium size remains nearly constant during sporulation, some resources should still be allocated to mycelial growth in order to compensate mycelial decay), contrary to saprophytic fungi (obtaining

nutrients from dead organic matter), for which optimal allocation strategies are purely bang-bang according to the results of [21]. Game-theoretic extensions of such dynamic models are worth investigating, since they can help to describe possible evolutionary equilibria in the realistic situations where several pathogen cohorts (with different genotypes) compete with each other for common resources within one host.

For simplicity, we study one-seasonal dynamics of only two biotrophic fungal cohorts within one host plant and assume constant lesion densities. From the perspective of Adaptive Dynamics, they can be interpreted as resident and mutant cohorts. The single state dynamic equation and corresponding optimization criterion in [15] are now replaced with two state dynamic equations and a suitable invasion functional (in the form of the difference between the two marginal fitness criteria). In both equations and both marginal fitnesses, there appears a so-called competition term that depends on both state variables if the lesion densities do not vanish. It is not clear what reasonable ways can be proposed in order to neglect the direct dependence of the resident dynamic equation and marginal fitness on the mutant state variable by assuming that the mutant lesion density is small in comparison with the resident one. Furthermore, competition between two pathogen cohorts with comparable lesion densities can be of interest by itself. These circumstances substantially complicate the use of the aforementioned two-step approach of [9–11] relying on Optimal Control Theory. Hence, we have to consider a zero-sum two-player differential game by employing the formulation of [11, §4.1]. Also note that, compared to optimal control problems, investigation of differential games turns out to be essentially more difficult [22–29] (a detailed mathematical discussion in connection with our problem will be given in Section 2).

Bearing in mind the general discussions in [11, 30], we do not have clear evidence of mutual cooperation between the resident and mutant populations. Those works point out that, in case when residents treat mutants as cooperators and keep using a collective optimal control strategy, the mutants refusing to cooperate in such a way may invade and eventually outcompete the residents. It is therefore reasonable to consider uninvadable and evolutionary stable strategies.

The paper is organized as follows. Section 2 provides a detailed statement of the problem. In Section 3, we analytically investigate the zero-sum two-cohort differential game. A number of important properties are rigorously derived. However, the complete theoretical analysis still remains an open challenging problem due to the high complexity of the differential game. That is why an ad hoc conjecture has to be additionally proposed. An informal but rather convincing and practical justification for the latter is given in Section 4 and based on numerical simulation results. Section 5 presents some asymptotic properties. In Section 6, we summarize the obtained analytical and numerical results together with their biological interpretations. The paper is also supported by electronic supplementary material consisting of two appendices. In [Online Appendix A](#), we recall the central results of the previous work [15] regarding the optimal control problem for a single cohort (compared to [15]),

slightly refined formulations and some new properties are provided). This helps to better understand similar reasoning in Subsection 3.3.1. [Online Appendix B](#) accompanies the investigation in Subsections 3.2 and 3.3.2.2.

## 2 Problem statement

### 2.1 Dynamic model

Consider one-seasonal dynamics of two biotrophic fungal cohorts within one host plant. Let us refer to them as to cohorts 1 and 2. For cohort  $i$ , denote the lesion density, *i. e.*, the number of mycelia per unit area of the host, by  $n_i$ . For simplicity, we assume that  $n_1, n_2$  are constant during the whole infection period within the season. This means that new infectious agents do not penetrate into the host during the observed period, *i. e.*, only the already present infections develop. Although this is in general a strong restriction for infections *in natura*, it still allows to obtain important results with relevant biological interpretations (as will be shown in the current work) and is reasonable in particular for experimental infection protocols (when, *e. g.*, a suspension of spores is sprayed on a leaf surface at a given date, and all related mycelia further develop in laboratory conditions and have almost the same age). Denote the average size of a mycelium in cohort  $i$  by  $M_i$ . Let  $S_i$  be the average quantity of spores produced by a mycelium in cohort  $i$ . The infection age  $t$  within the season is interpreted as a time variable.

The nutrient flux uptaken by cohort  $i$  is specified by a function  $f_i = f_i(M_1, M_2)$  and allocated between two different pathogen activities such as within-host multiplication (mycelial growth) and production of asexual spores. Let  $u_i = u_i(t)$  be a related resource allocation function taking values between zero and one. Adopt that the whole flux goes to mycelial growth when  $u_i(t) = 0$  and to spore production when  $u_i(t) = 1$ , while, for  $0 < u_i(t) < 1$ , there is an intermediate configuration. A similar approach to represent resource allocation functions was used in the model of [21] describing life-history strategies of saprophytic fungi, as well as in the general consumer-resource models studied in [11, 30, 31].

For both cohorts, let the rate of mycelial decay be determined by a function  $g = g(M)$ . Also suppose that, compared to mycelial growth, spores are produced with a constant yield  $\delta > 0$ .

The time span of the infections within the season is the interval  $[0, T]$ . The time horizon  $T > 0$  is fixed and can be finite or infinite. The infinite-horizon case is a reasonable abstraction when the pathogen dynamics is rather fast with respect to the whole infection duration. If  $T = +\infty$ , we understand  $[0, T]$  as  $[0, +\infty)$ .

Thus, we arrive at the following dynamic model:

$$\begin{cases} \frac{dM_1(t)}{dt} = (1 - u_1(t)) f_1(M_1(t), M_2(t)) - g(M_1(t)), \\ \frac{dM_2(t)}{dt} = (1 - u_2(t)) f_2(M_1(t), M_2(t)) - g(M_2(t)), \\ \frac{dS_1(t)}{dt} = \delta u_1(t) f_1(M_1(t), M_2(t)), \\ \frac{dS_2(t)}{dt} = \delta u_2(t) f_2(M_1(t), M_2(t)), \\ M_1(0) = M_1^0, \quad M_2(0) = M_2^0, \quad S_1(0) = S_1^0, \quad S_2(0) = S_2^0, \\ 0 \leq u_1(t) \leq 1, \quad 0 \leq u_2(t) \leq 1, \quad t \in [0, T]. \end{cases} \quad (1)$$

For brevity, we do not explicitly show dependence on the constant parameters  $n_1, n_2$  when writing  $f_i = f_i(M_1, M_2)$ ,  $i = 1, 2$ .

Since the right-hand sides of all four dynamic equations in (1) do not contain  $S_1, S_2$ , then we do not need to treat  $S_1, S_2$  explicitly, *i. e.*,  $M_1, M_2$  can be considered as the only state variables.

As in [15, Section 7], the mycelial sizes  $M_1, M_2$  can be measured in terms of equivalent amounts of infecting spores. In particular, if a mycelium appears from one spore at the beginning of the infection period, the initial mycelial size can be set as one equivalent of an infecting spore or, simply, as one spore. If one also measures time (infection age) in days and area of the host in  $\text{cm}^2$ , then the lesion densities  $n_1, n_2$  are measured in spores/ $\text{cm}^2$ , the nutrient fluxes  $f_1, f_2$  and the decay rate  $g$  are measured in spores/day, while the control variables  $u_1, u_2$  and the yield parameter  $\delta$  are dimensionless.

First, let us formulate the hypotheses that will be used all along the paper.

**Assumption 2.1** *The following holds:*

- 1)  $f_i = f_i(M_1, M_2)$ ,  $i = 1, 2$ , are twice continuously differentiable functions defined for all  $M_1 \geq 0$ ,  $M_2 \geq 0$  and taking nonnegative values;
- 2) for  $i = 1, 2$ , we have  $f_i(M_1, M_2) = 0$  if  $M_i = 0$ , and  $f_i(M_1, M_2) > 0$  if  $M_i > 0$ ;
- 3)  $g = g(M)$  is a twice continuously differentiable function defined for all  $M \geq 0$ ;
- 4)  $g(0) = 0$ , and  $g(M) > 0$  for  $M > 0$ ;
- 5) there exist sufficiently large numbers  $\bar{M}_1 > 0, \bar{M}_2 > 0$  such that

$$\begin{aligned} f_1(\bar{M}_1, M_2) - g(\bar{M}_1) &< 0 \quad \forall M_2 \in [0, \bar{M}_2], \\ f_2(M_1, \bar{M}_2) - g(\bar{M}_2) &< 0 \quad \forall M_1 \in [0, \bar{M}_1]. \end{aligned}$$

Assumption 2.1 implies that, for any initial coordinates  $M_i^0 \in (0, \bar{M}_i)$ ,  $i = 1, 2$ , and for any Lebesgue measurable functions  $u_i: [0, T] \rightarrow [0, 1]$ ,  $i = 1, 2$ , the system of the first two equations in (1) admits a unique trajectory  $[0, T] \ni t \mapsto (M_1(t), M_2(t)) \in \mathbb{R}^2$ , and

$$M_i(t) \in (0, \bar{M}_i) \quad \forall t \in [0, T], \quad i = 1, 2.$$

Hence, the domain

$$G \stackrel{\text{def}}{=} \{(M_1, M_2) \in \mathbb{R}^2 : 0 < M_1 < \bar{M}_1, 0 < M_2 < \bar{M}_2\} \quad (2)$$

is a bounded strongly invariant set in the state space for our controlled system [32, Chapter 4, §3].

The constants  $\bar{M}_1, \bar{M}_2$  can be interpreted as carrying capacity estimates.

Let us consider only the state trajectories that lie in the strongly invariant domain (2).

**Assumption 2.2**  $(M_1^0, M_2^0) \in G$ .

In the single-cohort case when one pathogen cohort is absent, the fitness criterion for remaining cohort  $i$  is specified as maximization of the lifetime reproductive success, which is a common definition of fitness in Ecology and Evolutionary Studies [33], and which can here be reduced to the expected reproductive output [34–36]. In line with [15, 21], the latter is characterized by  $\int_0^T (dS_i(t)/dt) e^{-\mu t} dt$ , where  $dS_i(t)/dt$  is the spore production rate at the infection age  $t$  (this rate in particular depends on the corresponding mycelial size  $M_i(t)$ ), and  $e^{-\mu t}$  is a term describing exponential extinction of the infections with a constant parameter  $\mu > 0$  (the probability density function of the related exponential distribution is determined as  $\mu e^{-\mu t}$  for all  $t \geq 0$ , and omitting the constant positive factor  $\mu$  leads to an equivalent criterion). In the double-cohort case governed by the system (1), this criterion is affected by both cohorts and can informally be written as

$$J_i(u_1(\cdot), u_2(\cdot)) \stackrel{\text{def}}{=} \int_0^T u_i(t) f_i(M_1(t), M_2(t)) e^{-\mu t} dt \longrightarrow \sup_{u_i(\cdot)}$$

(since  $\delta$  is a positive constant).

The next assumption represents some biological aspects of the model in more detail.

**Assumption 2.3** *The nutrient fluxes are determined by*

$$f_i(M_1, M_2) \stackrel{\text{def}}{=} \nu(n_1 M_1 + n_2 M_2) \cdot \rho(M_i) \quad \forall M_1 \geq 0 \quad \forall M_2 \geq 0, \quad i = 1, 2, \quad (3)$$

where the function  $\rho: [0, +\infty) \rightarrow [0, +\infty)$  specifies the resource flows that can be obtained by a single mycelium, and the function  $\nu: [0, +\infty) \rightarrow (0, +\infty)$  describes the negative influence of competition between mycelia for host resources. Moreover,  $\rho(\cdot), \nu(\cdot)$  are twice continuously differentiable on  $[0, +\infty)$ ,  $\rho(0) = 0$ , and  $\rho(M) > 0$  for  $M > 0$ .

The functions (3) satisfy  $f_1(M, M) = f_2(M, M)$  for all  $M \geq 0$ , which yields the property that  $J_1(u_1(\cdot), u_2(\cdot)) = J_2(u_1(\cdot), u_2(\cdot))$  if  $M_1^0 = M_2^0$  and Lebesgue measurable functions  $u_i: [0, T] \rightarrow [0, 1]$ ,  $i = 1, 2$ , are equivalent (*i. e.*, equal to each other almost everywhere on the time interval  $[0, T]$  with respect to Lebesgue measure).

Depending on the sections below, the following properties of the functions  $\nu(\cdot), \rho(\cdot), g(\cdot)$  will also be imposed.

**Assumption 2.4** Denote

$$\begin{aligned}\bar{M}_{\min} &\stackrel{\text{def}}{=} \min(\bar{M}_1, \bar{M}_2), & \bar{M}_{\max} &\stackrel{\text{def}}{=} \max(\bar{M}_1, \bar{M}_2), \\ n &\stackrel{\text{def}}{=} n_1 + n_2.\end{aligned}$$

The following conditions hold:

- 1)  $\nu'(x) \leq 0$  for  $x \in [0, n_1\bar{M}_1 + n_2\bar{M}_2]$ ;
- 2)  $\rho'(M) \geq 0$  and  $\rho''(M) \leq 0$  for  $M \in [0, \bar{M}_{\max}]$ ;
- 3)  $g'(M) \geq 0$  and  $g''(M) \geq 0$  for  $M \in [0, \bar{M}_{\max}]$ ;
- 4) either  $\nu(\cdot), \rho'(\cdot)$  are nonzero everywhere on  $(0, n_1\bar{M}_1 + n_2\bar{M}_2)$  and  $(0, \bar{M}_{\max})$ , respectively, or  $\rho''(\cdot)$  is nonzero everywhere on  $(0, \bar{M}_{\max})$ ;
- 5) in the degenerate case  $n = 0$ , we adopt that  $\rho''(M) < 0$  for  $M \in (0, \bar{M}_{\max})$ ;
- 6)  $\nu(0) \cdot \rho'(0) - g'(0) > \mu$ ;
- 7) there exists  $\tilde{M} \in (0, \bar{M}_{\min})$  such that

$$\nu(n\tilde{M}) \cdot \rho'(\tilde{M}) - g'(\tilde{M}) < \mu.$$

**Assumption 2.5** In the items 1–3 of Assumption 2.4, the intervals are extended up to  $+\infty$ , its items 4,5 are replaced merely with negativity of  $\rho''(\cdot)$  on  $(0, +\infty)$  regardless of  $n$ , and, in its item 7,  $\tilde{M} \in (0, \bar{M}_{\min})$  is replaced with  $\tilde{M} > 0$ .

**Assumption 2.6**  $\lim_{x \rightarrow +\infty} \nu(x) = 0$ , and  $\rho'(\cdot)$  is bounded on  $[0, +\infty)$ .

*Remark 2.7* In particular, the items 1–3 of Assumption 2.4 imply the following:

- $\nu(\cdot)$  is nonincreasing on  $[0, n_1\bar{M}_1 + n_2\bar{M}_2]$  (which is reasonable for the competition term with a growth reduction property);
- $\rho(\cdot)$  is nondecreasing and concave on  $[0, \bar{M}_{\max}]$  (a typical example is the classical Michaelis–Menten law [37] with a saturating growth behavior, as given in Example 2.8 below);
- $g(\cdot)$  is nondecreasing and convex on  $[0, \bar{M}_{\max}]$  (which holds for the linear decay rate given in Example 2.8 below).

Furthermore, the items 4–7 of Assumption 2.4 will also be required in Subsection 3.1, and Assumptions 2.5, 2.6 will be used in Section 5.  $\square$

Other assumptions will be formulated when needed in the subsequent sections.

Besides, we will also use Dieudonné’s notation:

$$\begin{aligned}D_i f_j &\stackrel{\text{def}}{=} \frac{\partial f_j}{\partial M_i}, & D_i[f_j - f_l] &\stackrel{\text{def}}{=} \frac{\partial(f_j - f_l)}{\partial M_i}, \\ D_{ij} f_l &\stackrel{\text{def}}{=} \frac{\partial^2 f_l}{\partial M_i \partial M_j}, & D_{ij}[f_l - f_q] &\stackrel{\text{def}}{=} \frac{\partial^2(f_l - f_q)}{\partial M_i \partial M_j}, \\ i = \overline{1, 2}, & \quad j = \overline{1, 2}, \quad l = \overline{1, 2}, \quad q = \overline{1, 2}.\end{aligned}\tag{4}$$

*Example 2.8* Introduce positive constants  $\alpha, k, \beta, \gamma$  and let

$$\rho(M) = \alpha \frac{M}{M+k} \quad \forall M \geq 0, \quad (5)$$

$$\nu(n_1 M_1 + n_2 M_2) = \frac{1}{1 + \beta(n_1 M_1 + n_2 M_2)} \quad \forall M_1 \geq 0 \quad \forall M_2 \geq 0, \quad (6)$$

$$g(M) = \gamma M \quad \forall M \geq 0. \quad (7)$$

Let

$$\alpha > k(\gamma + \mu). \quad (8)$$

Then  $\hat{M} \stackrel{\text{def}}{=} \alpha/\gamma - k$  is a unique positive root of the equation

$$\rho(\hat{M}) - g(\hat{M}) = \hat{M} \left( \frac{\alpha}{\hat{M} + k} - \gamma \right) = 0,$$

and, by taking  $\bar{M}_1 = \bar{M}_2 > \hat{M}$ , we satisfy the item 5 of Assumption 2.1, while its other items and Assumption 2.3 trivially hold. Assumptions 2.4–2.6 can also be verified easily. In particular, the item 6 of Assumption 2.4 follows directly from (8), and, in order to satisfy the inequality in its item 7, one can choose  $\tilde{M} = \hat{M}$ , since

$$\begin{aligned} \nu(n\hat{M}) \rho'(\hat{M}) - g'(\hat{M}) &= \frac{1}{1 + \beta n \hat{M}} \alpha \frac{k}{(\hat{M} + k)^2} - \gamma \\ &\leq \alpha \frac{k}{(\hat{M} + k)^2} - \gamma = \frac{k\gamma^2}{\alpha} - \gamma < \gamma - \gamma = 0. \quad \square \end{aligned}$$

*Example 2.9* Let  $\alpha, \beta, \gamma$  be positive constants. Consider the functions (6),(7) and also the linear function

$$\rho(M) = \alpha M \quad \forall M \geq 0$$

instead of (5). Then the nutrient fluxes (3) take the form

$$f_i(M_1, M_2) \stackrel{\text{def}}{=} \frac{\alpha M_i}{1 + \beta(n_1 M_1 + n_2 M_2)} \quad \forall M_1 \geq 0 \quad \forall M_2 \geq 0. \quad (9)$$

Suppose that  $n_1 > 0$ ,  $n_2 > 0$ , and  $\alpha > \gamma + \mu$ . It is not difficult to verify Assumptions 2.1, 2.3, 2.4, 2.6, but the condition that  $\rho''(M) < 0$  for all  $M > 0$  as imposed in Assumption 2.5 does not hold. Even though the nutrient fluxes (9) may seem to be more reasonable than those in Example 2.8, this is in fact not the case, as will be shown in Remark 5.2 below.  $\square$

*Remark 2.10* For simplicity, the nutrient concentration does not explicitly appear as one more variable in our model. However, the limitation of nutrient resources can be taken into account by imposing appropriate conditions on the functions  $\nu(\cdot), \rho(\cdot), g(\cdot)$  (see Remark 2.7 and Example 2.8). In particular, some biologically relevant asymptotic properties will be obtained in Section 5.

A separate differential equation for the nutrient concentration variable was incorporated in the model of [38] describing life history evolution of biotrophic wheat fungal pathogens. The sensitivity of the latent infection period and certain fitness measures with respect to a number of parameters (in other words, with respect to different fertilization scenarios) was numerically studied. However, the consideration was restricted to bang-bang resource allocation strategies, while singular regimes with coexisting spore production and maintenance of mycelia could be reasonable for many types of biotrophic fungal pathogens, as we already mentioned in the introduction. Furthermore, competition between two or more pathogen cohorts using different resource allocation strategies was not studied in [38]. Developing novel consumer-resource type models that combine some aspects of the models in [38] and in the current work is therefore a relevant subject of future research.  $\square$

For convenience, Table 1 lists the introduced variables, constant parameters, and functions constituting the fluxes in our dynamic model together with the corresponding measurement units. The parameters in the representations (5)–(7) are included as well.

For obtaining the numerical simulation results presented in the subsequent sections and in [Online Appendix A](#), the representations (5)–(7) and the following parameter values were used:

$$\begin{aligned} \alpha &= 0.2 \cdot 10^4 \text{ spores/day}, & k &= (1/6) \cdot 10^4 \text{ spores}, \\ \beta &= 10^{-5} \text{ cm}^2/\text{spores}^2, & \gamma &= 0.06 \text{ day}^{-1}, & \mu &= 0.03 \text{ day}^{-1}, & (10) \\ n_1 &= 9 \text{ spores/cm}^2, & n_2 &= 1 \text{ spore/cm}^2, & n &= 10 \text{ spores/cm}^2. \end{aligned}$$

Some comments on the selected parameter values can be found in [15, Section 7]. Note in particular that the values of  $\alpha, k, \gamma, \mu$  in (10) satisfy the inequality (8).

For brevity, the indicated measurement units will henceforth be omitted in the paper (one will be able to easily retrieve them with the help of Table 1).

## 2.2 Zero-sum two-cohort differential game and uninvadable strategies

The work [15] investigated the single-cohort optimal control problem

$$\begin{cases} \frac{dM(t)}{dt} = (1 - u(t))f(M(t)) - g(M(t)), & M(0) = M_0, \\ 0 \leq u(t) \leq 1, & t \in [0, T], \end{cases} \quad (11)$$

$$\int_0^T u(t) f(M(t)) e^{-\mu t} dt \longrightarrow \max, \quad (12)$$

where

$$f(M) \stackrel{\text{def}}{=} \nu(nM) \rho(M) \quad \forall M \geq 0, \quad n = \text{const} \geq 0$$

Variables/ Functions/ Parameters	Description	Measurement units
$t$	infection age (time variable)	days
$M_1, M_2$	average mycelium sizes in cohorts 1,2 (state variables)	spore equivalents or, simply, spores (this convention is used hereafter)
$S_1, S_2$	average quantities of spores produced per mycelium in cohorts 1,2	spores
$u_1, u_2$	resource allocation fractions for cohorts 1,2 (control variables)	dimensionless
$n_1, n_2$	lesion densities for cohorts 1,2	spores/cm <sup>2</sup>
$f_1(M_1, M_2),$ $f_2(M_1, M_2)$	nutrient fluxes for cohorts 1,2	spores/day
$g(M_1), g(M_2)$	mycelial decay rates for cohorts 1,2	spores/day
$\nu(n_1 M_1 + n_2 M_2)$	competition term in the nutrient fluxes	dimensionless
$\rho(M_1), \rho(M_2)$	specific resource flow terms in the nutrient fluxes	spores/day
$T$	time horizon	days
$\delta$	sporulation yield parameter	dimensionless
$\mu$	parameter in the dimensionless term $e^{-\mu t}$ describing exponential extinction of the infections	day <sup>-1</sup>
$\alpha$	rate constant in the particular representation (5) of $\rho(\cdot)$	spores/day
$k$	half-saturation constant in the particular representation (5) of $\rho(\cdot)$	spores
$\beta$	scaling parameter in the particular representation (6) of $\nu(\cdot)$	cm <sup>2</sup> /spores <sup>2</sup>
$\gamma$	decay rate parameter in the linear representation (7) of $g(\cdot)$	day <sup>-1</sup>

**Table 1** The variables, constant parameters, and functions constituting the fluxes in the proposed dynamic model together with the corresponding measurement units.

(see [Online Appendix A](#) including slightly refined formulations and some new properties).

In case of two pathogen cohorts, we employ the general theoretical framework of [11, § 4.1] and study one-seasonal competition between the cohorts in terms of their average reproductive outputs by seeking the saddle control strategies of a suitable class in the following zero-sum two-player differential game:

$$\begin{cases} \frac{dM_1(t)}{dt} = (1 - u_1(t)) f_1(M_1(t), M_2(t)) - g(M_1(t)), \\ \frac{dM_2(t)}{dt} = (1 - u_2(t)) f_2(M_1(t), M_2(t)) - g(M_2(t)), \\ M_1(0) = M_1^0, \quad M_2(0) = M_2^0, \\ 0 \leq u_1(t) \leq 1, \quad 0 \leq u_2(t) \leq 1, \quad t \in [0, T], \end{cases} \quad (13)$$

$$J(u_1(\cdot), u_2(\cdot)) \longrightarrow \inf_{u_1(\cdot)} \sup_{u_2(\cdot)} \text{ or } \sup_{u_2(\cdot)} \inf_{u_1(\cdot)}, \quad (14)$$

$$\begin{aligned}
J(u_1(\cdot), u_2(\cdot)) &\stackrel{\text{def}}{=} J_2(u_1(\cdot), u_2(\cdot)) - J_1(u_1(\cdot), u_2(\cdot)) \\
&= \int_0^T (u_2(t) f_2(M_1(t), M_2(t)) - u_1(t) f_1(M_1(t), M_2(t))) e^{-\mu t} dt. \quad (15)
\end{aligned}$$

For zero-sum two-player differential games, various concepts of lower and upper value functions, saddle points, and Nash equilibrium are called forth by various classes of control strategies, such as:

- 1) open-loop strategies [22, 39–44];
- 2) Varaiya–Roxin–Elliott–Kalton (VREK) or, simply, nonanticipative strategies [22, 45–48];
- 3) state-feedback or, more precisely, nonstationary state-feedback strategies [23–29, 49].

Let us explain the approach of [11, § 4.1] to define uninvadable and evolutionary stable strategies and how it relates to our differential game statement.

From the perspective of Adaptive Dynamics, let us interpret cohort 1 as a resident and cohort 2 as a mutant. Denote the corresponding classes of considered strategies as  $\mathcal{U}_1$  and  $\mathcal{U}_2$ . For a pair of strategies  $(u_1, u_2) \in \mathcal{U}_1 \times \mathcal{U}_2$ , we agree that the resident is not invaded by the mutant if and only if

$$J(u_1, u_2) \stackrel{\text{def}}{=} J_2(u_1, u_2) - J_1(u_1, u_2) \leq 0.$$

A strategy  $\hat{u}_1 \in \mathcal{U}_1$  is therefore uninvadable if and only if

$$J(\hat{u}_1, u_2) \leq 0 \quad \forall u_2 \in \mathcal{U}_2,$$

which is equivalent to

$$\sup_{u_2 \in \mathcal{U}_2} J(\hat{u}_1, u_2) \leq 0.$$

Such a  $\hat{u}_1$  exists if

$$\inf_{u_1 \in \mathcal{U}_1} \sup_{u_2 \in \mathcal{U}_2} J(u_1, u_2) = \min_{u_1 \in \mathcal{U}_1} \sup_{u_2 \in \mathcal{U}_2} J(u_1, u_2) \leq 0 \quad (16)$$

or

$$\inf_{u_1 \in \mathcal{U}_1} \sup_{u_2 \in \mathcal{U}_2} J(u_1, u_2) < 0 \quad (17)$$

(the latter inequality is mentioned in order to include the case when the infimum with respect to  $u_1$  is not reached). This motivates the game-theoretic statement (13)–(15), where the first player tries to maximize its resistance to an invasion by the second one, and vice versa. If  $M_1^0 = M_2^0$  and  $\mathcal{U}_1 = \mathcal{U}_2 = \mathcal{U}$ , then  $J(u, u) = 0$  for all  $u \in \mathcal{U}$ , (17) cannot hold, and (16) is simplified to the equality

$$\min_{u_1 \in \mathcal{U}} \sup_{u_2 \in \mathcal{U}} J(u_1, u_2) = 0.$$

In this case, a strategy

$$\hat{u}_1 \in \text{Arg min}_{u_1 \in \mathcal{U}} \left( \sup_{u_2 \in \mathcal{U}} J(u_1, u_2) \right)$$

is an ESS if the related maximum with respect to  $u_2$  is unique:

$$\text{Arg max}_{u_2 \in \mathcal{U}} J(\hat{u}_1, u_2) = \{\hat{u}_1\}.$$

Technically, these considerations are not totally rigorous for the classes of state-feedback strategies, since the corresponding lower and upper game values have to be defined by using specific mathematical constructions or hypotheses [23–28]. However, we can still adopt that a state-feedback strategy of cohort 1 is uninvadable if it gives the minimum in an appropriately defined upper (inf-sup) value of the game (13)–(15) and this value is nonpositive. Similarly, a state-feedback strategy of cohort 2 is said to be uninvadable if it gives the maximum in the related lower (sup-inf) value of the game (13)–(15) and this value is nonnegative. The same can be noted for the classes of nonanticipative strategies together with the corresponding lower and upper game values [22, 48].

Thus, the aim to find uninvadable or evolutionary stable strategies of the pathogen cohorts leads to the differential game (13)–(15).

If a saddle pair of open-loop control strategies exists, then, under standard technical assumptions, it satisfies Pontryagin’s minimax (or maximin) principle [22, § 3.3]. Some sufficient conditions for existence of saddle open-loop control strategies were given in [39–44]. However, they are rather strict and cannot be applied to the game (13)–(15).

Let  $V_{\text{VREK}}^-$  and  $V_{\text{VREK}}^+$  be the lower and upper value functions for the game (13)–(15) in the sense of nonanticipative strategies, respectively. Also let  $V_{\text{s-f}}^-$  and  $V_{\text{s-f}}^+$  be the lower and upper value functions for (13)–(15) that arise from the consideration of limit behavior of step-by-step control procedures based on state-feedback strategies [28, § III.11]. These functions are defined for  $(t, M_1, M_2) \in [0, T] \times G$  (since the states are restricted to lie in the strongly invariant domain  $G$ ). The Hamiltonian

$$\begin{aligned} H(t, M_1, M_2, u_1, u_2, p_1, p_2) &\stackrel{\text{def}}{=} p_1 ((1 - u_1) f_1(M_1, M_2) - g(M_1)) \\ &+ p_2 ((1 - u_2) f_2(M_1, M_2) - g(M_2)) + e^{-\mu t} (u_2 f_2(M_1, M_2) - u_1 f_1(M_1, M_2)) \quad (18) \\ \forall t \in [0, T] \quad \forall (M_1, M_2) \in G \quad \forall (u_1, u_2) \in [0, 1]^2 \quad \forall (p_1, p_2) \in \mathbb{R}^2 \end{aligned}$$

for (13)–(15) obviously satisfies the Isaacs condition

$$\begin{aligned} &\min_{u_1 \in [0, 1]} \max_{u_2 \in [0, 1]} H(t, M_1, M_2, u_1, u_2, p_1, p_2) \\ &= \max_{u_2 \in [0, 1]} \min_{u_1 \in [0, 1]} H(t, M_1, M_2, u_1, u_2, p_1, p_2) \stackrel{\text{def}}{=} \mathcal{H}(t, M_1, M_2, p_1, p_2) \\ &\forall t \in [0, T] \quad \forall (M_1, M_2) \in G \quad \forall (p_1, p_2) \in \mathbb{R}^2 \end{aligned}$$

( $p_1$  and  $p_2$  are the adjoint variables or, in other words, costates). Then, according to [48, §XI.6], the functions  $V_{\text{VREK}}^-, V_{\text{VREK}}^+$  coincide with each other and with the unique viscosity solution  $V: [0, T] \times G \rightarrow \mathbb{R}$  to the following Cauchy problem for the Hamilton–Jacobi–Isaacs (or, in short, HJI) equation:

$$\begin{cases} -\frac{\partial V(t, M_1, M_2)}{\partial t} - \mathcal{H}\left(t, M_1, M_2, \frac{\partial V(t, M_1, M_2)}{\partial M_1}, \frac{\partial V(t, M_1, M_2)}{\partial M_2}\right) = 0, \\ V(T, M_1, M_2) = 0, \quad (M_1, M_2) \in G, \quad t \in [0, T]. \end{cases} \quad (19)$$

Due to [28, Theorem III.11.4 and § I.4], we have  $V_{s-f}^- = V_{s-f}^+ = V$ , and this is also the unique minimax solution to the problem

$$\begin{cases} \frac{\partial V(t, M_1, M_2)}{\partial t} + \mathcal{H}\left(t, M_1, M_2, \frac{\partial V(t, M_1, M_2)}{\partial M_1}, \frac{\partial V(t, M_1, M_2)}{\partial M_2}\right) = 0, \\ V(T, M_1, M_2) = 0, \quad (M_1, M_2) \in G, \quad t \in [0, T] \end{cases} \quad (20)$$

(several equivalent definitions of minimax solutions can be found in [28, § I.3, I.4, II.6, II.7]).

In the particular case when  $V$  is continuously differentiable everywhere on  $[0, T] \times G$ , the saddle state-feedback control strategies can be constructed from the inclusions

$$\begin{aligned} u_1(t, M_1, M_2) &\in \operatorname{Arg} \min_{w_1 \in [0,1]} \left\{ \max_{w_2 \in [0,1]} H\left(t, M_1, M_2, w_1, w_2, \right. \right. \\ &\quad \left. \left. \frac{\partial V(t, M_1, M_2)}{\partial M_1}, \frac{\partial V(t, M_1, M_2)}{\partial M_2}\right)\right\}, \\ u_2(t, M_1, M_2) &\in \operatorname{Arg} \max_{w_2 \in [0,1]} \left\{ \min_{w_1 \in [0,1]} H\left(t, M_1, M_2, w_1, w_2, \right. \right. \\ &\quad \left. \left. \frac{\partial V(t, M_1, M_2)}{\partial M_1}, \frac{\partial V(t, M_1, M_2)}{\partial M_2}\right)\right\} \end{aligned}$$

$$\forall t \in [0, T] \quad \forall (M_1, M_2) \in G$$

(see [28, § III.11.5]), which are simplified to

$$\begin{aligned} u_1(t, M_1, M_2) &= \begin{cases} 0, & e^{-\mu t} + \frac{\partial V(t, M_1, M_2)}{\partial M_1} < 0, \\ 1, & e^{-\mu t} + \frac{\partial V(t, M_1, M_2)}{\partial M_1} > 0, \\ \text{arbitrary from } [0, 1], & e^{-\mu t} + \frac{\partial V(t, M_1, M_2)}{\partial M_1} = 0, \end{cases} \\ u_2(t, M_1, M_2) &= \begin{cases} 0, & e^{-\mu t} - \frac{\partial V(t, M_1, M_2)}{\partial M_2} < 0, \\ 1, & e^{-\mu t} - \frac{\partial V(t, M_1, M_2)}{\partial M_2} > 0, \\ \text{arbitrary from } [0, 1], & e^{-\mu t} - \frac{\partial V(t, M_1, M_2)}{\partial M_2} = 0, \end{cases} \quad (21) \end{aligned}$$

$$\forall t \in [0, T] \quad \forall (M_1, M_2) \in G.$$

Thus, the nonanticipative and state-feedback formulations of the differential game (13)–(15) are reduced to the Cauchy problem for the nonlinear first-order partial differential equation (19) or (20). One possible way to investigate this problem is to obtain the global field of its characteristics [23, 25, 26, 28, 29]. The method of characteristics (or, more precisely, an extension of the classical Cauchy method) is closely related to Pontryagin's principle, but some important features have to be emphasized. Contrary to optimal control problems, Pontryagin's principle for zero-sum two-player differential games provides necessary conditions only for saddle open-loop strategies, but not for saddle state-feedback strategies. The main qualitative difference in the behavior of characteristics for optimal control problems and differential games lies in the so-called corner conditions on switching manifolds [23–26]. While Pontryagin's theorem extends to Optimal Control Theory the Weierstrass–Erdmann condition stating that the adjoint function is continuous along an extremal trajectory, Differential Game Theory does not exclude discontinuities there.

These singularities in general cannot be found by a local analysis along isolated characteristics and require the construction of a complete field of extremals, leading to a global synthesis map. Recall also significant difficulties in verifying the existence of saddle open-loop strategies, as opposed to the well-known general result on the existence of saddle state-feedback strategies [27, 49].

Our aim is to investigate the Cauchy problem (19) for the HJI equation by the method of characteristics in order to describe the corresponding state-feedback control strategies, and then to give reasonable biological interpretations. It is also useful to compare the related analytical results with the results of solving this problem by an entirely numerical method such as finite-difference approximation [48, 50–52]. This can serve as a heuristic practical verification of our theoretical conjectures, while complete rigorous analysis of the global field of characteristics turns out to be very difficult.

### 3 Investigation of the zero-sum two-cohort differential game via the method of characteristics

From now on, Dieudonné's notation (4) will be actively used.

As was already mentioned in Section 2, the value function  $V_{\text{VREK}}^- = V_{\text{VREK}}^+ = V_{\text{s-f}}^- = V_{\text{s-f}}^+$  for the differential game (13)–(15) is described by the Cauchy problem (19) (or (20)) for the HJI equation in the finite-horizon case. Let us investigate this problem for  $T < +\infty$  by the method of characteristics [23, 25, 26, 28, 29]. Although Pontryagin's minimax principle [22, §3.3] is in general not a necessary condition for a saddle pair of nonanticipative or state-feedback control strategies, the corresponding characteristic (state dynamic and adjoint) equations

$$\begin{cases} \frac{dM_1(t)}{dt} = (1 - u_1(t)) f_1(M_1(t), M_2(t)) - g(M_1(t)), \\ \frac{dM_2(t)}{dt} = (1 - u_2(t)) f_2(M_1(t), M_2(t)) - g(M_2(t)), \end{cases} \quad (22)$$

$$\begin{cases} \frac{dp_1(t)}{dt} = - \frac{\partial H(t, M_1(t), M_2(t), u_1(t), u_2(t), p_1(t), p_2(t))}{\partial M_1} \\ \quad = p_1(t) (g'(M_1(t)) - (1 - u_1(t)) D_1 f_1(M_1(t), M_2(t))) \\ \quad \quad - p_2(t) (1 - u_2(t)) D_1 f_2(M_1(t), M_2(t)) \\ \quad \quad + e^{-\mu t} (u_1(t) D_1 f_1(M_1(t), M_2(t)) - u_2(t) D_1 f_2(M_1(t), M_2(t))), \\ \frac{dp_2(t)}{dt} = - \frac{\partial H(t, M_1(t), M_2(t), u_1(t), u_2(t), p_1(t), p_2(t))}{\partial M_2} \\ \quad = p_2(t) (g'(M_2(t)) - (1 - u_2(t)) D_2 f_2(M_1(t), M_2(t))) \\ \quad \quad - p_1(t) (1 - u_1(t)) D_2 f_1(M_1(t), M_2(t)) \\ \quad \quad + e^{-\mu t} (u_1(t) D_2 f_1(M_1(t), M_2(t)) - u_2(t) D_2 f_2(M_1(t), M_2(t))), \\ p_1(T) = p_2(T) = 0, \end{cases} \quad (23)$$

together with the Hamiltonian saddle-point condition

$$\begin{aligned} u_1(t) &\in \text{Arg} \min_{v_1 \in [0,1]} \left\{ \max_{v_2 \in [0,1]} H(t, M_1(t), M_2(t), v_1, v_2, p_1(t), p_2(t)) \right\}, \\ u_2(t) &\in \text{Arg} \max_{v_2 \in [0,1]} \left\{ \min_{v_1 \in [0,1]} H(t, M_1(t), M_2(t), v_1, v_2, p_1(t), p_2(t)) \right\} \end{aligned}$$

can still be used for the global analysis of (19), but not just for the analysis of isolated characteristics (recall the related discussion in the end of Section 2). With the help of the formula (18), the latter inclusions are simplified to

$$u_1(t) = \begin{cases} 0, & e^{-\mu t} + p_1(t) < 0, \\ 1, & e^{-\mu t} + p_1(t) > 0, \\ \text{arbitrary from } [0, 1], & e^{-\mu t} + p_1(t) = 0, \end{cases} \quad (24)$$

$$u_2(t) = \begin{cases} 0, & e^{-\mu t} - p_2(t) < 0, \\ 1, & e^{-\mu t} - p_2(t) > 0, \\ \text{arbitrary from } [0, 1], & e^{-\mu t} - p_2(t) = 0. \end{cases} \quad (25)$$

Since the boundary conditions for the adjoint variables  $p_1, p_2$  are imposed at  $t = T$ , it is convenient to rewrite (22)–(25) in reverse time  $\tau \stackrel{\text{def}}{=} T - t$ :

$$\begin{cases} \frac{dM_1}{d\tau} = g(M_1) - (1 - u_1) f_1(M_1, M_2), \\ \frac{dM_2}{d\tau} = g(M_2) - (1 - u_2) f_2(M_1, M_2), \end{cases} \quad (26)$$

$$\begin{cases} \frac{dp_1}{d\tau} = -p_1 g'(M_1) + p_1 D_1 f_1(M_1, M_2) + p_2 D_1 f_2(M_1, M_2) \\ \quad - (e^{-\mu(T-\tau)} + p_1) u_1 D_1 f_1(M_1, M_2) \\ \quad + (e^{-\mu(T-\tau)} - p_2) u_2 D_1 f_2(M_1, M_2), \\ \frac{dp_2}{d\tau} = -p_2 g'(M_2) + p_1 D_2 f_1(M_1, M_2) + p_2 D_2 f_2(M_1, M_2) \\ \quad - (e^{-\mu(T-\tau)} + p_1) u_1 D_2 f_1(M_1, M_2) \\ \quad + (e^{-\mu(T-\tau)} - p_2) u_2 D_2 f_2(M_1, M_2), \\ p_1|_{\tau=0} = p_2|_{\tau=0} = 0, \end{cases} \quad (27)$$

$$u_1 = \begin{cases} 0, & e^{-\mu(T-\tau)} + p_1 < 0, \\ 1, & e^{-\mu(T-\tau)} + p_1 > 0, \\ \text{arbitrary from } [0, 1], & e^{-\mu(T-\tau)} + p_1 = 0, \end{cases} \quad (28)$$

$$u_2 = \begin{cases} 0, & e^{-\mu(T-\tau)} - p_2 < 0, \\ 1, & e^{-\mu(T-\tau)} - p_2 > 0, \\ \text{arbitrary from } [0, 1], & e^{-\mu(T-\tau)} - p_2 = 0. \end{cases} \quad (29)$$

Here the time argument for  $M_1, M_2, u_1, u_2, p_1, p_2$  is not shown for brevity.

The formulas (28),(29) together with the boundary conditions for the adjoint system (27) directly imply that  $u_1 = u_2 = 1$  for sufficiently small  $\tau$  (or, equivalently, for  $t$  sufficiently close to  $T$ ).

### 3.1 Singular control regimes for both cohorts

First, let us study the situation when, on some time subinterval, we have  $e^{-\mu(T-\tau)} + p_1 = e^{-\mu(T-\tau)} - p_2 = 0$ , *i. e.*, when singular control regimes take place simultaneously for both cohorts.

From (27), we get

$$\begin{aligned} & \frac{d}{d\tau} \left( e^{-\mu(T-\tau)} + p_1 \right) \Big|_{e^{-\mu(T-\tau)} + p_1 = 0} \\ &= -e^{-\mu(T-\tau)} (D_1 f_1(M_1, M_2) - g'(M_1) - \mu) \\ & \quad + p_2 D_1 f_2(M_1, M_2) + \left( e^{-\mu(T-\tau)} - p_2 \right) u_2 D_1 f_2(M_1, M_2), \end{aligned} \quad (30)$$

$$\begin{aligned} & \frac{d}{d\tau} \left( e^{-\mu(T-\tau)} - p_2 \right) \Big|_{e^{-\mu(T-\tau)} - p_2 = 0} \\ &= -e^{-\mu(T-\tau)} (D_2 f_2(M_1, M_2) - g'(M_2) - \mu) \\ & \quad - p_1 D_2 f_1(M_1, M_2) + \left( e^{-\mu(T-\tau)} + p_1 \right) u_1 D_2 f_1(M_1, M_2), \end{aligned} \quad (31)$$

and, therefore,

$$\begin{aligned} & \frac{d}{d\tau} \left( e^{-\mu(T-\tau)} + p_1 \right) \Big|_{e^{-\mu(T-\tau)} + p_1 = e^{-\mu(T-\tau)} - p_2 = 0} \\ & \quad = -e^{-\mu(T-\tau)} (D_1[f_1 - f_2](M_1, M_2) - g'(M_1) - \mu), \\ & \frac{d}{d\tau} \left( e^{-\mu(T-\tau)} - p_2 \right) \Big|_{e^{-\mu(T-\tau)} + p_1 = e^{-\mu(T-\tau)} - p_2 = 0} \\ & \quad = -e^{-\mu(T-\tau)} (D_2[f_2 - f_1](M_1, M_2) - g'(M_2) - \mu). \end{aligned}$$

Thus, singular control regimes can appear simultaneously for the two cohorts only when

$$D_1[f_1 - f_2](M_1, M_2) - g'(M_1) = D_2[f_2 - f_1](M_1, M_2) - g'(M_2) = \mu. \quad (32)$$

Due to the form of the nutrient fluxes given in Assumption 2.3, the equations (32) transform into

$$\begin{aligned} & n_1 \nu'(n_1 M_1 + n_2 M_2) (\rho(M_1) - \rho(M_2)) + \nu(n_1 M_1 + n_2 M_2) \rho'(M_1) - g'(M_1) \\ &= n_2 \nu'(n_1 M_1 + n_2 M_2) (\rho(M_2) - \rho(M_1)) + \nu(n_1 M_1 + n_2 M_2) \rho'(M_2) - g'(M_2) \quad (33) \\ &= \mu. \end{aligned}$$

Denote

$$\begin{aligned} n &\stackrel{\text{def}}{=} n_1 + n_2, \\ f(M) &\stackrel{\text{def}}{=} f_1(M, M) = f_2(M, M) = \nu(nM) \rho(M) \quad \forall M \geq 0. \end{aligned}$$

For establishing the next result on the concurrent singular control regimes, one also needs the properties of the functions  $\nu(\cdot), \rho(\cdot), g(\cdot)$  from Assumption 2.4.

**Theorem 3.1** *Suppose that  $T < +\infty$  and Assumptions 2.1–2.4 hold. The system of equations (33) with respect to  $(M_1, M_2)$  has a unique solution  $(M^{**}, M^{**}) \in G$ , where  $M^{**}$  is a unique root of the equation*

$$\nu(nM^{**})\rho'(M^{**}) - g'(M^{**}) = \mu \quad (34)$$

on  $(0, \bar{M}_{\min})$ . Consider a solution to the reverse-time characteristic system (26)–(29) with  $(M_1, M_2)|_{\tau=0} \in G$  on the maximum subinterval of  $[0, T]$  where the state stays in  $G$ . Singular control regimes may take place simultaneously for both cohorts only when  $M_1 = M_2 = M^{**}$  and  $u_1 = u_2 = u^{**} \in [0, 1]$ , where

$$u^{**} \stackrel{\text{def}}{=} 1 - \frac{g(M^{**})}{f(M^{**})}. \quad (35)$$

Moreover, if  $\bar{M}_1 = \bar{M}_2 \stackrel{\text{def}}{=} \bar{M}$  and the equation

$$\begin{aligned} f'(M^*) - g'(M^*) \\ = n\nu'(nM^*)\rho(M^*) + \nu(nM^*)\rho'(M^*) - g'(M^*) = \mu \end{aligned} \quad (36)$$

has a unique root  $M^* \in (0, \bar{M})$  (which is related to singular arcs in the optimal control problem (11),(12) according to Assumption A.2 and Proposition A.3 in [Online Appendix A](#)), then

$$\begin{aligned} M^* \leq M^{**}, \\ (n > 0, \nu'(nM^*) < 0) \implies (M^* < M^{**}). \end{aligned} \quad (37)$$

*Proof* From the equations (33), we obtain

$$\begin{aligned} n\nu'(n_1M_1 + n_2M_2)(\rho(M_2) - \rho(M_1)) \\ + \nu(n_1M_1 + n_2M_2)(\rho'(M_2) - \rho'(M_1)) + (g'(M_1) - g'(M_2)) = 0. \end{aligned}$$

With the help of the items 1–5 of Assumption 2.4, one can directly verify that, in the domain (2), this equality can hold only for  $M_1 = M_2$  (its left-hand side is negative for  $M_1 < M_2$  and positive for  $M_1 > M_2$ ). Then the system (33) is reduced to one equation (34). By using the items 1–5 of Assumption 2.4 again, we get

$$\begin{aligned} \frac{\partial}{\partial M} (\nu(nM)\rho'(M) - g'(M)) \\ = n\nu'(nM)\rho'(M) + \nu(nM)\rho''(M) - g''(M) < 0 \\ \forall M \in (0, \bar{M}_{\max}). \end{aligned} \quad (38)$$

Together with the final items 6,7, this leads to the existence of a unique root  $M^{**}$  of (34) on  $(0, \bar{M}_{\min})$ . Thus,  $(M^{**}, M^{**})$  is a unique solution to (33) in  $G$ , and the control strategies  $u_1, u_2$  may act in singular regimes simultaneously only when  $M_1 = M_2 = M^{**}$  and  $u_1 = u_2 = u^{**} \in [0, 1]$ .

It remains to verify the properties (37). From the equations (34),(36) together with the item 1 of Assumption 2.4, we obtain

$$\nu(nM^*)\rho'(M^*) - g'(M^*) \geq \nu(nM^{**})\rho'(M^{**}) - g'(M^{**}). \quad (39)$$

According to (38), this implies  $M^* \leq M^{**}$ . If we also have  $n > 0$  and  $\nu'(nM^*) < 0$ , then the inequality (39) becomes strict and, therefore,  $M^* < M^{**}$ .  $\square$

*Remark 3.2* The inequality  $M^* < M^{**}$  means that, in comparison with the singular control regime in the single-cohort optimization problem, maintaining the singular control regime for both cohorts in the zero-sum differential game requires greater resources.  $\square$

The next assumption is imposed in order to have  $0 < u^{**} < 1$ , *i. e.*, an intermediate configuration of resource allocation in the singular control regime for the two cohorts.

**Assumption 3.3**  $f(M^{**}) > g(M^{**})$ .

*Example 3.4* Let  $n \geq 0$ , and let the representations (5)–(7) hold with positive constants  $\alpha, k, \beta, \gamma$  satisfying the inequality (8). Then Assumptions 2.1, 2.3–2.6 are fulfilled (see Example 2.8). Assumption 2.2 is trivial and supposed to hold *a priori*. Hence, Theorem 3.1 can be applied. If  $n > 0$ , then  $\nu'(\cdot)$  is negative on  $[0, +\infty)$  and, by virtue of (37),  $M^* < M^{**}$ . Finally, note that (34) transforms into

$$\frac{1}{1 + \beta n M^{**}} \alpha \frac{k}{(M^{**} + k)^2} = \gamma + \mu,$$

which implies fulfillment of Assumption 3.3:

$$f(M^{**}) = \frac{1}{1 + \beta n M^{**}} \frac{\alpha M^{**}}{M^{**} + k} = (\gamma + \mu) M^{**} \frac{M^{**} + k}{k} > \gamma M^{**} = g(M^{**}).$$

Therefore, the singular control (35) is admissible and specifies an intermediate configuration of resource allocation.  $\square$

### 3.2 Characteristics in case $M_1|_{\tau=0} \neq M_2|_{\tau=0}$

In this subsection, we need to adopt the linear form (7) for the function  $g(\cdot)$ .

**Assumption 3.5**  $g(M) = \gamma M$  for all  $M \geq 0$ ,  $\gamma$  is a positive constant.

The next theorem describes important properties of solutions to the reverse-time characteristic system (26)–(29) in case  $M_1|_{\tau=0} \neq M_2|_{\tau=0}$  (or, equivalently,  $M_1|_{t=T} \neq M_2|_{t=T}$ ).

**Theorem 3.6** *Suppose that  $T < +\infty$  and Assumptions 2.1–2.4, 3.5 hold. Consider a solution to the reverse-time characteristic system (26)–(29) with  $(M_1, M_2)|_{\tau=0} \in G$  on the maximum subinterval  $I \subseteq [0, T]$  where the state stays in  $G$ . Let  $\mathcal{T}$  be the right endpoint of  $I$  (in fact,  $I = [0, T]$  if  $\mathcal{T} = T$  and  $(M_1, M_2)|_{\tau=T} \in G$ , otherwise  $I = [0, \mathcal{T})$ ). Fix an arbitrary instant  $\tau' \in [0, \mathcal{T})$  and denote*

$$[\tau', \mathcal{T}] \stackrel{\text{def}}{=} [\tau', T] \cap I, \quad (\tau', \mathcal{T}) \stackrel{\text{def}}{=} (\tau', T) \cap I$$

(where } is either ] or ) depending on  $I$ ). Then the following implications hold:

$$\begin{aligned} (M_1|_{\tau=\tau'} > M_2|_{\tau=\tau'}, \quad (p_1 + p_2)|_{\tau=\tau'} \geq 0) \\ \implies (M_1 > M_2 \quad \forall \tau \in [\tau', \mathcal{T}], \quad p_1 + p_2 > 0 \quad \forall \tau \in (\tau', \mathcal{T})), \end{aligned}$$

$$\begin{aligned} (M_1|_{\tau=\tau'} < M_2|_{\tau=\tau'}, \quad (p_1 + p_2)|_{\tau=\tau'} \leq 0) \\ \implies (M_1 < M_2 \quad \forall \tau \in [\tau', \mathcal{T}], \quad p_1 + p_2 < 0 \quad \forall \tau \in (\tau', \mathcal{T})). \end{aligned}$$

In the particular case  $\tau' = 0$ , we have

$$\begin{aligned} (M_1|_{\tau=0} > M_2|_{\tau=0}) \\ \implies (M_1 > M_2 \quad \forall \tau \in [0, \mathcal{T}], \quad p_1 + p_2 > 0 \quad \forall \tau \in (0, \mathcal{T})), \end{aligned} \quad (40)$$

$$\begin{aligned} (M_1|_{\tau=0} < M_2|_{\tau=0}) \\ \implies (M_1 < M_2 \quad \forall \tau \in [0, \mathcal{T}], \quad p_1 + p_2 < 0 \quad \forall \tau \in (0, \mathcal{T})). \end{aligned} \quad (41)$$

Theorem 3.6 is proved in Section B.1 of [Online Appendix B](#).

*Remark 3.7* Consider a solution to the characteristic system (26)–(29) for  $\tau \in [0, \mathcal{T}]$  under the conditions of Theorem 3.6. Recall that  $u_1 = u_2 = 1$  for sufficiently small  $\tau$  (i. e., for  $t$  sufficiently close to  $T$ ). If  $M_1|_{\tau=0} > M_2|_{\tau=0}$ , then, due to (40), we have  $e^{-\mu(T-\tau)} + p_1 > e^{-\mu(T-\tau)} - p_2$  for all  $\tau \in (0, \mathcal{T}]$ , which, in particular, implies that, in reverse time, the first switching of  $u_1$  may happen only after the first switching of  $u_2$  (i. e., in forward time, the last switching of  $u_2$  may happen only after the last switching of  $u_1$ ). Similarly, if  $M_1|_{\tau=0} < M_2|_{\tau=0}$ , then, due to (41),  $e^{-\mu(T-\tau)} + p_1 < e^{-\mu(T-\tau)} - p_2$  for all  $\tau \in (0, \mathcal{T}]$ , which, in particular, implies that, in reverse time, the first switching of  $u_2$  may happen only after the first switching of  $u_1$  (i. e., in forward time, the last switching of  $u_1$  may happen only after the last switching of  $u_2$ ).  $\square$

### 3.3 Characteristics in case $M_1|_{\tau=0} = M_2|_{\tau=0}$

In this subsection, we study solutions to the characteristic system (26)–(29) in case  $M_1|_{\tau=0} = M_2|_{\tau=0}$ .

#### 3.3.1 Staying on the plane $M_1 = M_2$

First, it is reasonable to describe the field of characteristics staying on the plane  $M_1 = M_2$  under the action of equal control strategies  $u_1 = u_2$ . Then we arrive at the following system for  $M_1 = M_2 = M$ ,  $-p_1 = p_2 = p$ ,  $u_1 = u_2 = u$ :

$$\begin{cases} \frac{dM}{d\tau} = g(M) - (1-u)f(M), \\ \frac{dp}{d\tau} = -pg'(M) + \left(p + \left(e^{-\mu(T-\tau)} - p\right)u\right) \nu(nM) \rho'(M), \\ p|_{\tau=0} = 0, \\ u = \begin{cases} 0, & e^{-\mu(T-\tau)} - p < 0, \\ 1, & e^{-\mu(T-\tau)} - p > 0, \\ \text{arbitrary from } [0, 1], & e^{-\mu(T-\tau)} - p = 0. \end{cases} \end{cases} \quad (42)$$

It can be investigated similarly to the characteristic system for the optimal control problem (11),(12) (the latter is studied in [Online Appendix A](#)). That is why we omit the proofs of Proposition 3.9 and Theorem 3.11 below.

For the analysis of the system (42), we do not need linearity of  $g(\cdot)$ , *i. e.*, Assumption 3.5. The latter will be required further, when applying Theorem 3.6 to the reverse-time characteristics that leave the plane  $M_1 = M_2$ .

Here we impose a stronger condition than  $f(M^{**}) > g(M^{**})$  in Assumption 3.3, and also positivity of  $\rho'(M^{**})$ .

**Assumption 3.8**  $f(M) > g(M)$  for all  $M \in (0, M^{**}]$ , and  $\rho'(M^{**}) > 0$ .

According to the item 2 of Assumption 2.4, the inequality  $\rho'(M^{**}) > 0$  implies that

$$\rho'(M) > 0 \quad \forall M \in [0, M^{**}]. \quad (43)$$

Similarly to [Online Appendix A](#), we will indicate the feedback control law for the system (42) on the plane  $(t, M)$ .

For describing the set of bang-bang switchings on the plane  $(t, M)$ , we need an auxiliary notation, as in Proposition A.6 of [Online Appendix A](#). Fix arbitrary  $\tau' \geq 0$  and  $M' \in (0, \bar{M}_{\min})$ . Let us write the state dynamic equation from the system (42) in reverse time for  $u \equiv 1$ :

$$\frac{dM}{d\tau} = g(M).$$

By  $\eta(\cdot; \tau', M')$ , denote its solution considered for  $\tau \leq \tau'$  and reaching  $M = M'$  at  $\tau = \tau'$ . Since this differential equation is autonomous, we have  $\eta(\tau; \tau', M') = \eta(-(\tau' - \tau); 0, M')$  for all  $\tau \leq \tau'$ . In case  $M' = 0$ , we trivially set  $\eta(\tau; \tau', 0) = 0$  for all  $\tau \leq \tau'$  (because  $g(0) = 0$  in line with the item 4 of Assumption 2.1).

**Proposition 3.9** *Suppose that  $T < +\infty$  and Assumptions 2.1–2.4, 3.3, 3.8 hold. On the plane  $(t, M)$ , the bang-bang switching set for the system (42) can be represented as*

$$\tilde{\Gamma}_{\text{b-b}} = \left\{ (t, M) \in (-\infty, T] \times [0, M^{**}] : \tilde{\lambda}_{\text{b-b}}(T - t, M) = 0 \right\},$$

where

$$\tilde{\lambda}_{\text{b-b}}(\tau, M) \stackrel{\text{def}}{=} 1 - \int_0^\tau \exp \left\{ - \int_0^s g'(\eta(-\xi; 0, M)) d\xi - \mu s \right\} \cdot \nu(n \eta(-s; 0, M)) \rho'(\eta(-s; 0, M)) ds \quad (44)$$

$$\forall \tau \geq 0 \quad \forall M \in [0, \bar{M}_{\min}).$$

For  $M \neq 0$ , the formula (44) can be simplified to

$$\tilde{\lambda}_{\text{b-b}}(\tau, M) = 1 - \frac{1}{g(M)} \int_0^\tau e^{-\mu s} g(\eta(-s; 0, M)) \nu(n \eta(-s; 0, M)) \rho'(\eta(-s; 0, M)) ds$$

$$\forall \tau \geq 0 \quad \forall M \in (0, \bar{M}_{\min}),$$

as in Remark A.8 of [Online Appendix A](#).

From the relations (43),(44) and the fact that  $0 \leq \eta(-\tau; 0, M) \leq M$  for all  $\tau \geq 0$  and  $M \in [0, \bar{M}_{\min})$ , we get

$$\begin{aligned} \frac{\partial \tilde{\lambda}_{\text{b-b}}(\tau, M)}{\partial \tau} &= -\exp \left\{ -\int_0^\tau g'(\eta(-\xi; 0, M)) d\xi - \mu\tau \right\} \\ &\quad \cdot \nu(n \eta(-\tau; 0, M)) \rho'(\eta(-\tau; 0, M)) < 0 \\ \forall \tau \geq 0 \quad \forall M \in [0, M^{**}]. \end{aligned} \quad (45)$$

The role of the next assumption is similar to the role of Assumption A.7 in [Online Appendix A](#).

**Assumption 3.10** *For any  $M \in (0, M^{**}]$ , there exists a number  $\tau > 0$  satisfying  $\tilde{\lambda}_{\text{b-b}}(\tau, M) = 0$ , or, equivalently,*

$$\begin{aligned} \int_0^{+\infty} e^{-\mu s} g(\eta(-s; 0, M)) \nu(n \eta(-s; 0, M)) \rho'(\eta(-s; 0, M)) ds &> g(M) \\ \forall M \in (0, M^{**}]. \end{aligned} \quad (46)$$

Similarly to the reasoning in the end of Remark A.8 in [Online Appendix A](#), one can use the formula (44) and the item 6 of Assumption 2.4 in order to show that the case  $M = 0$  does not need to be included in Assumption 3.10.

The inequality (45) implies uniqueness of  $\tau$  in Assumption 3.10 and also the fact that  $\tilde{\Gamma}_{\text{b-b}}$  is a regular curve. In particular, there exists a unique  $\tau^{**} > 0$  satisfying  $\tilde{\lambda}_{\text{b-b}}(\tau^{**}, M^{**}) = 0$ . Furthermore, if we consider the curve  $\tilde{\Gamma}_{\text{b-b}}$  in reverse time, then it will not depend on the finite time horizon  $T$ . The numbers  $M^{**}, \tau^{**}$  are also independent from  $T$ .

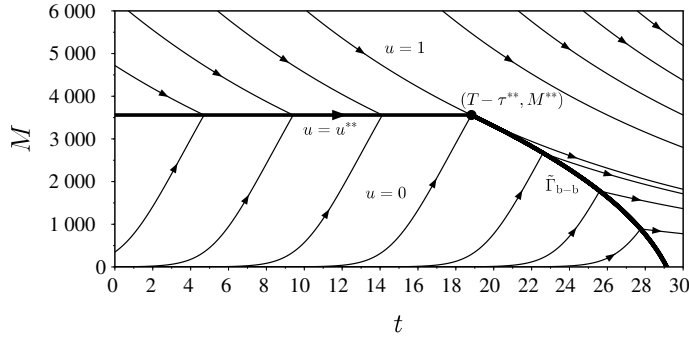
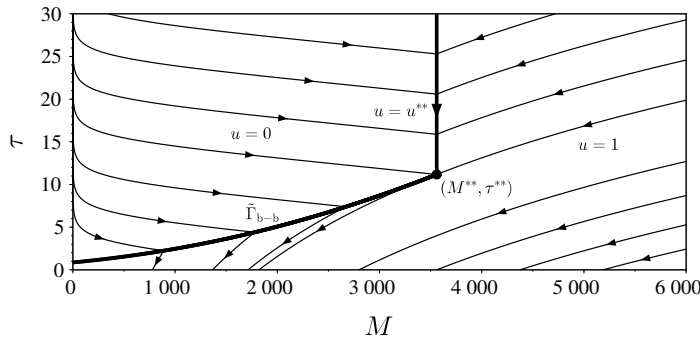
Similarly to Assumption A.7 in [Online Appendix A](#), analytical verification of Assumption 3.10 may be rather complicated, but a practical test for the corresponding condition (46) is naturally implemented within the numerical construction of  $\tilde{\Gamma}_{\text{b-b}}$ , when computing zeros of (44).

Similarly to Remark A.11 in [Online Appendix A](#), Assumptions 2.1–2.4, 3.3, 3.8, 3.10 guarantee transversal crossing of the bang-bang switching curve  $\tilde{\Gamma}_{\text{b-b}}$  by the characteristic arcs of (42) with  $u = 0$ .

The above notation allows us to formulate a result on the structure of the feedback control strategy for the system (42) (recall Theorem A.12 in [Online Appendix A](#) and see also Fig. 2a).

**Theorem 3.11** *Suppose that  $T < +\infty$  and Assumptions 2.1–2.4, 3.3, 3.8, 3.10 hold. The field of the characteristics staying on the plane  $M_1 = M_2$  and governed by the system (42) determines the following feedback control strategy:*

$$\begin{aligned} u(t, M) &= \begin{cases} 1, & 0 < M < M^{**}, \tilde{\lambda}_{\text{b-b}}(T-t, M) \geq 0, \\ 0, & 0 < M < M^{**}, \tilde{\lambda}_{\text{b-b}}(T-t, M) < 0, \\ u^{**}, & M = M^{**}, 0 \leq t < T - \tau^{**}, \\ 1, & M = M^{**}, T - \tau^{**} \leq t \leq T, \\ 1, & M > M^{**}, \end{cases} \\ \forall t \in [0, T] \quad \forall M \in (0, \bar{M}_{\min}). \end{aligned} \quad (47)$$

a) The portrait on the plane  $(t, M)$ b) The portrait on the plane  $(M, \tau)$ 

**Fig. 2** The feedback control law (47) for the time horizon  $T = 30$ , functions (5)–(7), and parameter values (10). The portrait is drawn (a) on the plane  $(t, M)$  and (b) on the plane  $(M, \tau)$ . The arrows on the trajectories correspond to the forward time directions.

Fig. 2a illustrates the constructed feedback control law for the time horizon  $T = 30$ , functions (5)–(7), and parameter values (10) (which satisfy Assumptions 2.1, 2.3–2.6, 3.3, 3.5, 3.8, 3.10). For further reverse-time considerations, it is also useful to draw the related portrait of characteristics on the plane  $(M, \tau)$ , as done in Fig. 2b (where the arrows on the trajectories still correspond to the forward time directions).

### 3.3.2 Exit from the plane $M_1 = M_2$

The next step is to describe the reverse-time characteristics that start from  $M_1|_{\tau=0} = M_2|_{\tau=0}$  and leave the plane  $M_1 = M_2$  when reaching suitable positions. This leaving can happen only as a result of such control switchings that make  $u_1 \neq u_2$  without violation of the Hamiltonian saddle-point condition (28), (29). The above analysis of the system (42) implies that it is possible

to stop staying on the plane  $M_1 = M_2$  only at the positions

$$\begin{aligned} (\tau, M_1, M_2, p_1, p_2) &= \left( \tau', M^{**}, M^{**}, -e^{-\mu(T-\tau')}, e^{-\mu(T-\tau')} \right), \\ \tau^{**} &\leq \tau' < T. \end{aligned} \quad (48)$$

Suppose that  $\tau^{**} < T$ , and let  $\tau' \in [\tau^{**}, T)$  be such an exit instant. Then, in some right neighborhood of  $\tau = \tau'$ , the following regimes are possible:

- 1)  $u_1 = 1$ ,  $u_2$  is singular,  $M_1 > M_2$ ,  $e^{-\mu(T-\tau)} + p_1 > 0$ ,  $e^{-\mu(T-\tau)} - p_2 = 0$ ,  $p_1 + p_2 > 0$ ;
- 2)  $u_1$  is singular,  $u_2 = 1$ ,  $M_1 < M_2$ ,  $e^{-\mu(T-\tau)} + p_1 = 0$ ,  $e^{-\mu(T-\tau)} - p_2 > 0$ ,  $p_1 + p_2 < 0$ ;
- 3)  $u_1$  is singular,  $u_2 = 0$ ,  $M_1 > M_2$ ,  $e^{-\mu(T-\tau)} + p_1 = 0$ ,  $e^{-\mu(T-\tau)} - p_2 < 0$ ,  $p_1 + p_2 > 0$ ;
- 4)  $u_1 = 0$ ,  $u_2$  is singular,  $M_1 < M_2$ ,  $e^{-\mu(T-\tau)} + p_1 < 0$ ,  $e^{-\mu(T-\tau)} - p_2 = 0$ ,  $p_1 + p_2 < 0$ ;
- 5)  $u_1 = 1$ ,  $u_2 = 0$ ,  $M_1 > M_2$ ,  $e^{-\mu(T-\tau)} + p_1 > 0$ ,  $e^{-\mu(T-\tau)} - p_2 < 0$ ,  $p_1 + p_2 > 0$ ;
- 6)  $u_1 = 0$ ,  $u_2 = 1$ ,  $M_1 < M_2$ ,  $e^{-\mu(T-\tau)} + p_1 < 0$ ,  $e^{-\mu(T-\tau)} - p_2 > 0$ ,  $p_1 + p_2 < 0$ .

Let Assumption 3.5 hold in addition to  $T < +\infty$  and Assumptions 2.1–2.4, 3.3, 3.8, 3.10. By using Theorem 3.6, we conclude that, if the regime 1, 3, or 5 takes place in some right neighborhood of  $\tau = \tau'$ , then  $M_1 > M_2$  and  $p_1 + p_2 > 0$  for all  $\tau \in (\tau', \mathcal{T})$ . Similarly, if the regime 2, 4, or 6 takes place in some right neighborhood of  $\tau = \tau'$ , then  $M_1 < M_2$  and  $p_1 + p_2 < 0$  for all  $\tau \in (\tau', \mathcal{T})$ .

The regular regimes 5 and 6 do not need to be separately investigated, because the corresponding control values are known *a priori*. Let us characterize the singular control components for the regimes 1–4.

### 3.3.2.1 Singular control regimes 1–4

**Regime 1.** By virtue of the representation (31), we have

$$\begin{aligned} \frac{d}{d\tau} \left( e^{-\mu(T-\tau)} - p_2 \right) \Big|_{e^{-\mu(T-\tau)} - p_2 = 0, u_1 = 1} \\ = -e^{-\mu(T-\tau)} (D_2[f_2 - f_1](M_1, M_2) - g'(M_2) - \mu), \end{aligned}$$

which implies

$$D_2[f_2 - f_1](M_1, M_2) - g'(M_2) - \mu = 0 \quad (49)$$

due to singularity of the control  $u_2$ . By differentiating the last equality with respect to  $\tau$  subject to the state dynamic equations (26) for  $u_1 = 1$ , we can find the corresponding feedback control law  $u_2 = u_2(M_1, M_2)$ :

$$\begin{aligned} D_{12}[f_2 - f_1](M_1, M_2) g(M_1) + (D_{22}[f_2 - f_1](M_1, M_2) - g''(M_2)) \\ \cdot (g(M_2) - (1 - u_2) f_2(M_1, M_2)) = 0, \end{aligned} \quad (50)$$

$$\begin{aligned} & (1 - u_2) f_2(M_1, M_2) - g(M_2) \\ &= g(M_1) \frac{D_{12}[f_2 - f_1](M_1, M_2)}{D_{22}[f_2 - f_1](M_1, M_2) - g''(M_2)}. \end{aligned}$$

**Regime 2.** Similarly to the reasonings for the regime 1, we consecutively derive

$$D_1[f_1 - f_2](M_1, M_2) - g'(M_1) - \mu = 0, \quad (51)$$

$$\begin{aligned} D_{12}[f_1 - f_2] g(M_2) + (D_{11}[f_1 - f_2](M_1, M_2) - g''(M_1)) \\ \cdot (g(M_1) - (1 - u_1) f_1(M_1, M_2)) = 0, \end{aligned} \quad (52)$$

$$\begin{aligned} & (1 - u_1) f_1(M_1, M_2) - g(M_1) \\ &= g(M_2) \frac{D_{12}[f_1 - f_2](M_1, M_2)}{D_{11}[f_1 - f_2](M_1, M_2) - g''(M_1)}. \end{aligned}$$

**Regime 3.** From the representation (30), we get

$$\begin{aligned} & \frac{d}{d\tau} \left( e^{-\mu(T-\tau)} + p_1 \right) \Big|_{e^{-\mu(T-\tau)} + p_1 = 0, (e^{-\mu(T-\tau)} - p_2) u_2 = 0} \\ &= -e^{-\mu(T-\tau)} (D_1 f_1(M_1, M_2) - g'(M_1) - \mu) + p_2 D_1 f_2(M_1, M_2), \end{aligned}$$

*i. e.,*

$$p_2 D_1 f_2(M_1, M_2) - e^{-\mu(T-\tau)} (D_1 f_1(M_1, M_2) - g'(M_1) - \mu) = 0 \quad (53)$$

due to singularity of the control  $u_1$ . In the degenerate case  $n_1 = 0$ , we have  $D_1 f_2(M_1, M_2) \equiv 0$  and thereby arrive at the relations

$$D_1 f_1(M_1, M_2) - g'(M_1) - \mu = 0, \quad (54)$$

$$\begin{aligned} & (D_{11} f_1(M_1, M_2) - g''(M_1)) (g(M_1) - (1 - u_1) f_1(M_1, M_2)) \\ &+ D_{12} f_1(M_1, M_2) (g(M_2) - f_2(M_1, M_2)) = 0, \end{aligned} \quad (55)$$

$$\begin{aligned} & (1 - u_1) f_1(M_1, M_2) - g(M_1) \\ &= \frac{D_{12} f_1(M_1, M_2) (g(M_2) - f_2(M_1, M_2))}{D_{11} f_1(M_1, M_2) - g''(M_1)}. \end{aligned}$$

Now suppose that  $D_1 f_2(M_1, M_2) \neq 0$  on the considered subarc. Then (53) gives

$$p_2 = e^{-\mu(T-\tau)} \frac{D_1 f_1(M_1, M_2) - g'(M_1) - \mu}{D_1 f_2(M_1, M_2)}. \quad (56)$$

By differentiating (53) with respect to  $\tau$  subject to the equations (26),(27) for  $u_2 = 0$ , we obtain

$$\begin{aligned} & \frac{dp_2}{d\tau} D_1 f_2(M_1, M_2) + p_2 \left( D_{11} f_2(M_1, M_2) \frac{dM_1}{d\tau} + D_{12} f_2(M_1, M_2) \frac{dM_2}{d\tau} \right) \\ & - \mu e^{-\mu(T-\tau)} (D_1 f_1(M_1, M_2) - g'(M_1) - \mu) \\ & - e^{-\mu(T-\tau)} \left( (D_{11} f_1(M_1, M_2) - g''(M_1)) \frac{dM_1}{d\tau} + D_{12} f_1(M_1, M_2) \frac{dM_2}{d\tau} \right) = 0, \end{aligned}$$

$$\begin{aligned}
& \left( p_2 (D_2 f_2(M_1, M_2) - g'(M_2)) - e^{-\mu(T-\tau)} D_2 f_1(M_1, M_2) \right) \cdot D_1 f_2(M_1, M_2) \\
& + p_2 \left( D_{11} f_2(M_1, M_2) \frac{dM_1}{d\tau} + D_{12} f_2(M_1, M_2) \frac{dM_2}{d\tau} \right) \\
& - \mu e^{-\mu(T-\tau)} (D_1 f_1(M_1, M_2) - g'(M_1) - \mu) \\
& - e^{-\mu(T-\tau)} \left( (D_{11} f_1(M_1, M_2) - g''(M_1)) \frac{dM_1}{d\tau} + D_{12} f_1(M_1, M_2) \frac{dM_2}{d\tau} \right) = 0,
\end{aligned}$$

and, after substituting (56) and canceling  $e^{-\mu(T-\tau)}$ ,

$$\begin{aligned}
& \frac{dM_1}{d\tau} \left( \frac{D_{11} f_2(M_1, M_2) (D_1 f_1(M_1, M_2) - g'(M_1) - \mu)}{D_1 f_2(M_1, M_2)} \right. \\
& \quad \left. - D_{11} f_1(M_1, M_2) + g''(M_1) \right) \\
& + \frac{dM_2}{d\tau} \left( \frac{D_{12} f_2(M_1, M_2) (D_1 f_1(M_1, M_2) - g'(M_1) - \mu)}{D_1 f_2(M_1, M_2)} - D_{12} f_1(M_1, M_2) \right) \quad (57) \\
& - D_2 f_1(M_1, M_2) D_1 f_2(M_1, M_2) \\
& + (D_1 f_1(M_1, M_2) - g'(M_1) - \mu) (D_2 f_2(M_1, M_2) - g'(M_2) - \mu) = 0,
\end{aligned}$$

$$\begin{aligned}
& (1 - u_1) f_1(M_1, M_2) - g(M_1) \\
& = \left( \frac{D_{11} f_2(M_1, M_2) (D_1 f_1(M_1, M_2) - g'(M_1) - \mu)}{D_1 f_2(M_1, M_2)} \right. \\
& \quad \left. - D_{11} f_1(M_1, M_2) + g''(M_1) \right)^{-1} \\
& \cdot \left( (g(M_2) - f_2(M_1, M_2)) \right. \\
& \quad \cdot \left( \frac{D_{12} f_2(M_1, M_2) (D_1 f_1(M_1, M_2) - g'(M_1) - \mu)}{D_1 f_2(M_1, M_2)} - D_{12} f_1(M_1, M_2) \right) \\
& \quad \left. - D_2 f_1(M_1, M_2) D_1 f_2(M_1, M_2) \right. \\
& \quad \left. + (D_1 f_1(M_1, M_2) - g'(M_1) - \mu) (D_2 f_2(M_1, M_2) - g'(M_2) - \mu) \right).
\end{aligned}$$

**Regime 4.** Similarly to the reasonings for the regime 3, we consecutively derive

$$D_2 f_2(M_1, M_2) - g'(M_2) - \mu = 0, \quad (58)$$

$$\begin{aligned}
& (D_{22} f_2(M_1, M_2) - g''(M_2)) (g(M_2) - (1 - u_2) f_2(M_1, M_2)) \\
& + D_{12} f_2(M_1, M_2) (g(M_1) - f_1(M_1, M_2)) = 0, \quad (59)
\end{aligned}$$

$$\begin{aligned}
& (1 - u_2) f_2(M_1, M_2) - g(M_2) \\
& = \frac{D_{12} f_2(M_1, M_2) (g(M_1) - f_1(M_1, M_2))}{D_{22} f_2(M_1, M_2) - g''(M_2)}
\end{aligned}$$

in the degenerate case  $n_2 = 0$ , and

$$\begin{aligned} & \frac{dM_2}{d\tau} \left( \frac{D_{22}f_1(M_1, M_2) (D_2f_2(M_1, M_2) - g'(M_2) - \mu)}{D_2f_1(M_1, M_2)} \right. \\ & \quad \left. - D_{22}f_2(M_1, M_2) + g''(M_2) \right) \\ & + \frac{dM_1}{d\tau} \left( \frac{D_{12}f_1(M_1, M_2) (D_2f_2(M_1, M_2) - g'(M_2) - \mu)}{D_2f_1(M_1, M_2)} - D_{12}f_2(M_1, M_2) \right) \\ & - D_1f_2(M_1, M_2) D_2f_1(M_1, M_2) \\ & + (D_2f_2(M_1, M_2) - g'(M_2) - \mu) (D_1f_1(M_1, M_2) - g'(M_1) - \mu) = 0, \end{aligned} \quad (60)$$

$$\begin{aligned} & (1 - u_2) f_2(M_1, M_2) - g(M_2) \\ & = \left( \frac{D_{22}f_1(M_1, M_2) (D_2f_2(M_1, M_2) - g'(M_2) - \mu)}{D_2f_1(M_1, M_2)} \right. \\ & \quad \left. - D_{22}f_2(M_1, M_2) + g''(M_2) \right)^{-1} \\ & \cdot \left( (g(M_1) - f_1(M_1, M_2)) \right. \\ & \quad \cdot \left( \frac{D_{12}f_1(M_1, M_2) (D_2f_2(M_1, M_2) - g'(M_2) - \mu)}{D_2f_1(M_1, M_2)} - D_{12}f_2(M_1, M_2) \right) \\ & \quad \left. - D_1f_2(M_1, M_2) D_2f_1(M_1, M_2) \right. \\ & \quad \left. + (D_2f_2(M_1, M_2) - g'(M_2) - \mu) (D_1f_1(M_1, M_2) - g'(M_1) - \mu) \right) \end{aligned}$$

if  $D_2f_1(M_1, M_2) \neq 0$  on the considered subarc.

### 3.3.2.2 Stationary feedback control law

The next theoretical constructions are needed in order to describe the stationary feedback control law for such parts of the reverse-time characteristics that emanate from the positions (48) (and then either leave the plane  $M_1 = M_2$  at some  $\tau \in [\tau', T)$  or stay there till  $\tau = T$ ).

Consider the four reverse-time dynamical systems that are obtained from (26) by substituting the feedback control pairs for the studied regimes 1–4. Let us refer to them as the systems 1–4, respectively.

A number of additional assumptions have to be adopted.

**Assumption 3.12** *For every  $j \in \{1, 2, 3, 4\}$ , there exists a closed domain  $\bar{D}_j \subseteq \bar{G}$  such that  $(M^{**}, M^{**}) \in D_j \stackrel{\text{def}}{=} \text{int } \bar{D}_j$  and the right-hand side of the system  $j$  is defined and continuously differentiable in  $\bar{D}_j$ .*

For convenience, let  $\tau = 0$  be the initial instant for the systems 1–4 (since they are autonomous, one can choose an arbitrary initial instant for them, not necessarily  $\tau \geq \tau^{**}$ ), and set the initial condition as  $(M_1, M_2)|_{\tau=0} = (M^{**}, M^{**})$ . For every  $j \in \{1, 2, 3, 4\}$ , consider the resulting Cauchy problem

for the system  $j$  on the maximum extendability interval  $[0, \theta_j)$  until the first exit from the open domain  $D_j$  (the case  $\theta_j < +\infty$ ) or up to infinity (the case  $\theta_j = +\infty$ ) if there is no such an exit. Denote the related state trajectories by  $\Sigma_1$ – $\Sigma_4$ , respectively. Here we do not restrain the time intervals by the number  $T - \tau^{**}$ , because we want to make our constructions independent from a particular finite time horizon  $T$ .

The following assumption means that the singular control components for the regimes 1–4 correspond to intermediate configurations of resource allocation (this is rather typical for singular policies, while bang-bang policies take only boundary values).

**Assumption 3.13** *For every  $j \in \{1, 2, 3, 4\}$ , the singular control component for the regime  $j$  lies in  $(0, 1)$  on the state trajectory  $\Sigma_j$ .*

In Subsection B.2.1 of [Online Appendix B](#), the following properties of the curves  $\Sigma_1$ – $\Sigma_4$  are established under Assumptions [2.1–2.4](#), [3.3](#), [3.5](#), [3.8](#), [3.10](#), [3.12](#), [3.13](#) (for better understanding, it is useful to look at [Fig. 3](#) below in advance, that figure is related to the functions [\(5\)–\(7\)](#) and parameter values [\(10\)](#)):

- the state trajectories  $\Sigma_1$ – $\Sigma_4$  are regular curves located so that

$$\begin{aligned} (\Sigma_1 \cup \Sigma_3) \setminus \{(M^{**}, M^{**})\} &\subset \{(M_1, M_2) \in G : M_1 > M_2\}, \\ (\Sigma_2 \cup \Sigma_4) \setminus \{(M^{**}, M^{**})\} &\subset \{(M_1, M_2) \in G : M_1 < M_2\}; \end{aligned}$$

- the time bounds  $\theta_1, \theta_2$  for the state trajectories  $\Sigma_1, \Sigma_2$  are finite (however, general analytical verification of whether the time bounds  $\theta_3, \theta_4$  for the state trajectories  $\Sigma_3, \Sigma_4$  are finite or infinite remains an open problem);
- if  $j \in \{1, 2, 3, 4\}$  and  $\theta_j < +\infty$ , then the limit endpoint of  $\Sigma_j$  for  $\tau \nearrow \theta_j$  lies neither on the line  $M_1 = 0$  nor on the line  $M_2 = 0$ ;
- if  $j \in \{1, 3\}$ , then the limit endpoint of  $\Sigma_j$  for  $\tau \nearrow \theta_j$  belongs to the closed half-plane  $M_1 \geq M_2$ ;
- if  $j \in \{2, 4\}$ , then the limit endpoint of  $\Sigma_j$  for  $\tau \nearrow \theta_j$  belongs to the closed half-plane  $M_1 \leq M_2$ .

In line with the next assumption, all curves  $\Sigma_1$ – $\Sigma_4$  end on the boundary of  $G$ .

**Assumption 3.14** *For every  $j \in \{1, 2, 3, 4\}$ , the limit endpoint of the state trajectory  $\Sigma_j$  for  $\tau \nearrow \theta_j$  lies on the boundary  $\partial G$  of the domain [\(2\)](#).*

For describing the sought-after feedback control law, the following assumption plays a crucial role. In particular, it guarantees that the reverse-time characteristics do not have any switchings after exiting from the singular control regimes on the curves  $\Sigma_1$ – $\Sigma_4$ . This can be verified with the help of the same representations for the first and second derivatives of the switching functions  $e^{-\mu(T-\tau)} + p_1$ ,  $e^{-\mu(T-\tau)} - p_2$  and related expressions as were used in the above analysis of the regimes 1–4.

**Assumption 3.15** *The following conditions hold (see [Fig. 3b](#)):*

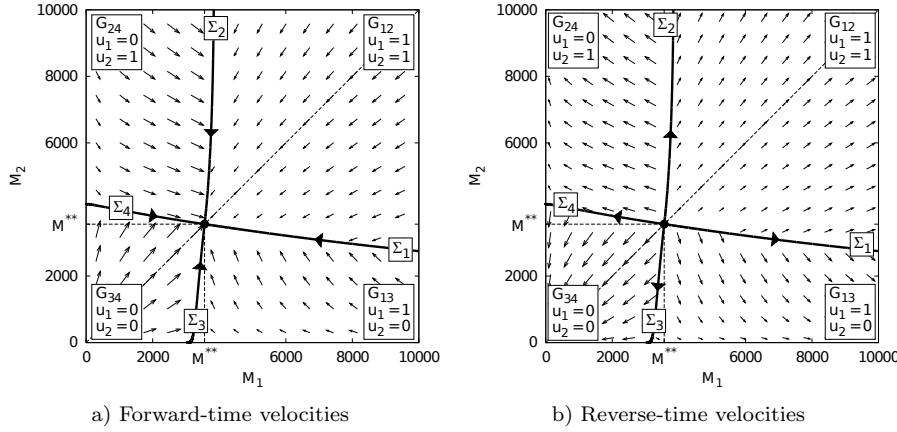


**Fig. 3** The feedback control law (61) for the functions (5)–(7) and parameter values (10). The velocities are drawn (a) in forward time and (b) in reverse time.

- 1) the sets  $\Sigma_j \setminus \{(M^{**}, M^{**})\}$ ,  $j = \overline{1, 4}$ , are mutually disjoint (which implies that the only common point of  $\Sigma_1$ – $\Sigma_4$  is  $(M^{**}, M^{**})$ );
- 2) the curves  $\Sigma_1$ – $\Sigma_4$  divide the strongly invariant region  $G$  into four open domains  $G_{12}, G_{13}, G_{24}, G_{34}$ , so that

$$G = \left( \bigcup_{j=1}^4 \Sigma_j \right) \cup G_{12} \cup G_{13} \cup G_{24} \cup G_{34}$$

and, for  $(j_1, j_2) = (1, 2), (1, 3), (2, 4), (3, 4)$ , the domain  $G_{j_1 j_2}$  is located between the curves  $\Sigma_{j_1}$  and  $\Sigma_{j_2}$ , i. e.,

$$\Sigma_{j_1} \cup \Sigma_{j_2} \subseteq \partial G_{j_1 j_2} \subseteq \Sigma_{j_1} \cup \Sigma_{j_2} \cup \partial G;$$

- 3) on  $\Sigma_1 \cup \Sigma_2$ , the vector of the right-hand side of the reverse-time system (26) with  $(u_1, u_2) = (1, 1)$  is directed strictly inside the domain  $G_{12}$ ;
- 4) on  $\Sigma_1 \cup \Sigma_3$ , the vector of the right-hand side of the reverse-time system (26) with  $(u_1, u_2) = (1, 0)$  is directed strictly inside the domain  $G_{13}$ ;
- 5) on  $\Sigma_2 \cup \Sigma_4$ , the vector of the right-hand side of the reverse-time system (26) with  $(u_1, u_2) = (0, 1)$  is directed strictly inside the domain  $G_{24}$ ;
- 6) on  $\Sigma_3 \cup \Sigma_4$ , the vector of the right-hand side of the reverse-time system (26) with  $(u_1, u_2) = (0, 0)$  is directed strictly inside the domain  $G_{34}$ ;
- 7) the left-hand side of (49) is negative in  $G_{12} \cup (\Sigma_2 \setminus \{(M^{**}, M^{**})\})$  and positive in  $G_{13} \cup (\Sigma_3 \setminus \{(M^{**}, M^{**})\})$ , the coefficient near  $u_2$  in (50) is negative on  $\Sigma_1$  (note that, under Assumption 3.5, negativity of this coefficient is equivalent to negativity of  $D_{22}[f_2 - f_1](M_1, M_2)$ );
- 8) the left-hand side of (51) is negative in  $G_{12} \cup (\Sigma_1 \setminus \{(M^{**}, M^{**})\})$  and positive in  $G_{24} \cup (\Sigma_4 \setminus \{(M^{**}, M^{**})\})$ , the coefficient near  $u_1$  in (52) is negative on  $\Sigma_2$  (note that, under Assumption 3.5, negativity of this coefficient is equivalent to negativity of  $D_{11}[f_1 - f_2](M_1, M_2)$ );

- 9) in the degenerate case  $n_1 = 0$ , the left-hand side of (54) is negative in  $G_{13}$  and positive in  $G_{34}$ , and the coefficient near  $u_1$  in (55) is negative on  $\Sigma_3$  (note that, under Assumption 3.5, negativity of this coefficient is equivalent to negativity of  $D_{11}f_1(M_1, M_2)$ );
- 10) if  $n_1 > 0$ , then the left-hand side of (57) with  $(dM_1/d\tau, dM_2/d\tau)$  determined by (26) with  $(u_1, u_2) = (1, 0)$  is positive in  $\Sigma_1 \cup \Sigma_3 \cup G_{13}$ , and, for  $(u_1, u_2) = (0, 0)$ , this expression is negative in  $\Sigma_3 \cup \Sigma_4 \cup G_{34}$ ;
- 11) in the degenerate case  $n_2 = 0$ , the left-hand side of (58) is negative in  $G_{24}$  and positive in  $G_{34}$ , and the coefficient near  $u_2$  in (59) is negative on  $\Sigma_4$  (note that, under Assumption 3.5, negativity of this coefficient is equivalent to negativity of  $D_{22}f_2(M_1, M_2)$ );
- 12) if  $n_2 > 0$ , then the left-hand side of (60) with  $(dM_1/d\tau, dM_2/d\tau)$  determined by (26) with  $(u_1, u_2) = (0, 1)$  is positive in  $\Sigma_2 \cup \Sigma_4 \cup G_{24}$ , and, for  $(u_1, u_2) = (0, 0)$ , this expression is negative in  $\Sigma_3 \cup \Sigma_4 \cup G_{34}$ .

*Remark 3.16* If a rigorous analytical verification of Assumptions 3.12–3.15 turns out to be very difficult, it is reasonable to check them informally, based on numerical approximations of the state trajectories  $\Sigma_1$ – $\Sigma_4$  (one-dimensional curvilinear grids) and domains  $G_{12}, G_{13}, G_{24}, G_{34}$  (two-dimensional grids). This has been done in the particular case of the functions (5)–(7) and parameter values (10), when obtaining the numerical results for Fig. 3.  $\square$

By using the above characterizations of the singular control regimes 1–4 and related state trajectories  $\Sigma_1$ – $\Sigma_4$  (dividing  $G$  into the subdomains  $G_{12}, G_{13}, G_{24}, G_{34}$ ), we directly arrive at the main result of this subsection (see also Fig. 3).

**Theorem 3.17** *Suppose that  $T < +\infty$  and Assumptions 2.1–2.4, 3.3, 3.5, 3.8, 3.10, 3.12–3.15 hold. The following representation describes the feedback control law for such parts of the reverse-time characteristics of (26)–(29) that emanate from the positions (48):*

$$(u_1(M_1, M_2), u_2(M_1, M_2)) = \begin{cases} (1, 1), & (M_1, M_2) \in G_{12}, \\ (1, 0), & (M_1, M_2) \in G_{13}, \\ (0, 1), & (M_1, M_2) \in G_{24}, \\ (0, 0), & (M_1, M_2) \in G_{34}. \end{cases}$$

Furthermore, the regime  $u_1 = u_2 = u^{**}$  should be applied for staying at  $M_1 = M_2 = M^{**}$ , and the regimes 1–4 should be used for staying on  $\Sigma_j \setminus \{(M^{**}, M^{**})\}$ ,  $j = \overline{1, 4}$ , respectively. When considering the characteristics in forward time, this feedback map becomes single-valued everywhere in  $G$  and

takes the form

$$(u_1(M_1, M_2), u_2(M_1, M_2)) = \begin{cases} (1, 1), & (M_1, M_2) \in G_{12}, \\ (1, 0), & (M_1, M_2) \in G_{13}, \\ (0, 1), & (M_1, M_2) \in G_{24}, \\ (0, 0), & (M_1, M_2) \in G_{34}, \\ (u^{**}, u^{**}), & M_1 = M_2 = M^{**}, \\ \text{as in the regime } j, & (M_1, M_2) \in \Sigma_j \setminus \{(M^{**}, M^{**})\}, \quad j = \overline{1, 4}. \end{cases} \quad (61)$$

Fig. 3 illustrates numerical approximations of the state trajectories  $\Sigma_1$ – $\Sigma_4$  and feedback control law (61) for the functions (5)–(7) and parameter values (10). We take  $\bar{M}_1 = \bar{M}_2 = \bar{M}$  as in Example 2.8. In the case (5)–(7), (10), we choose this bound as  $\bar{M} = 3.5 \cdot 10^4 > \hat{M} \approx 3.167 \cdot 10^4$ , which is much greater than  $M^{**} \approx 0.356 \cdot 10^4$ . In order to focus on the key aspects of the feedback map in a neighborhood of the point  $(M^{**}, M^{**})$ , we show the portrait only on a subdomain of  $G$ . The portrait on the remaining part of  $G$  is clear, and, in particular, the state trajectories  $\Sigma_1$  and  $\Sigma_2$  end on the lines  $M_1 = \bar{M}$  and  $M_2 = \bar{M}$ , respectively. On the lines  $M_2 = 0$  and  $M_1 = 0$ , one can see the limit endpoints of  $\Sigma_3$  and  $\Sigma_4$ , respectively. The fields of the forward-time and reverse-time velocities (*i. e.*, the vectors of the right-hand sides of the dynamical systems (22) and (26) with the substituted control law (61)) are also indicated in the two subfigures. The point  $(M^{**}, M^{**})$  appears to be an attractor for the considered parts of the forward-time characteristics.

*Remark 3.18* In Subsection B.2.2 of [Online Appendix B](#), it is proved that, under the conditions of Theorem 3.17, the singular feedback strategies  $u_2$  in the regimes 1, 4 and  $u_1$  in the regimes 2, 3 continuously join the value  $u^{**}$  at the state  $(M^{**}, M^{**})$  only if  $n_1 = n_2$  or  $\nu'((n_1 + n_2)M^{**}) = 0$  (which is a rather narrow case).  $\square$

Let the conditions of Theorem 3.17 hold. Then the curves  $\Sigma_i \setminus \{(M^{**}, M^{**})\}$ ,  $i = \overline{1, 4}$ , are universal manifolds, and there is no kind of “perpetuated dilemma”, contrary to equivocal manifolds [23, 29, 53]. Indeed, upon reaching any of these curves from the domain  $G_{12}$ ,  $G_{13}$ ,  $G_{24}$  or  $G_{34}$ , one cohort has to switch its control from 0 or 1 to the appropriate singular regime, while the other one keeps its control 0 or 1. The situation with entering the doubly singular regime  $u_1 = u_2 = u^{**}$  at the state  $(M^{**}, M^{**})$  (from any of the curves  $\Sigma_i \setminus \{(M^{**}, M^{**})\}$ ,  $i = \overline{1, 4}$ , or directly from  $G_{13} \cup G_{24}$ ) is much more complicated. In fact, these are junctions with a one-dimensional curve in a three-dimensional space (one has two state variables and a time variable), *i. e.*, junctions with a manifold of codimension 2. To our knowledge, a clear theory of such junctions is currently missing. The best hint we have for the correctness of our analytical constructions is a very good agreement with the switching surfaces obtained from a numerical solution of the Cauchy problem for the HJI equation (see Fig. 6 in Section 4 below).

### 3.4 Resulting conjecture on the structure of the saddle state-feedback control strategies in the infinite-horizon case

For drawing rigorous conclusions about the structure of the saddle state-feedback control strategies in case  $T < +\infty$ , the global portrait of the characteristics of the problem (19) has to be described. But, as opposed to the characteristics with  $M_1|_{\tau=0} = M_2|_{\tau=0}$ , complete analytical investigation of the field of the characteristics with  $M_1|_{\tau=0} \neq M_2|_{\tau=0}$  appears to be very difficult. In the coordinate space  $(M_1, M_2, \tau)$  with the vertical axis  $\tau$ , the latter are located below the characteristic arcs emanating from the positions (48). According to Theorem 3.6, the regions  $M_1 > M_2$  and  $M_1 < M_2$  are invariant for the reverse-time characteristics. Furthermore, Remark 3.7 specifies the order in which the characteristics with  $M_1|_{\tau=0} \neq M_2|_{\tau=0}$  may reach the corresponding switching surfaces. One can expect that there should be four such surfaces (two in each of the domains  $M_1 > M_2$  and  $M_1 < M_2$ ) and they continuously join the other switching surfaces generated by the singular control regimes 1–4 from Subsection 3.3.2. Even though this property has not been proved in our characteristic analysis, the numerical simulation results of the next section will give the related informal verification (see Fig. 7). It is also natural to observe that the reduction of the saddle state-feedback control map to the horizontal plane for a fixed time instant is determined by four domains and four separating curves, and, for sufficiently large  $T$  and  $\tau \stackrel{\text{def}}{=} T - t$ , the latter differ from  $\Sigma_1$ – $\Sigma_4$  only near the boundary  $\partial G$  (see Fig. 6). More precisely, this difference is likely to tend to zero as  $\tau \rightarrow +\infty$ , and there should even be exact coincidence with  $\Sigma_1$  for  $\tau \geq \tau^{**} + \theta_1$  and with  $\Sigma_2$  for  $\tau \geq \tau^{**} + \theta_2$  (finiteness of the time bounds  $\theta_1, \theta_2$  is one of the properties mentioned directly after Assumption 3.13).

Thus, we arrive at the conjecture that, in the infinite-horizon case  $T = +\infty$ , the saddle state-feedback control strategies should have the same stationary form (61) as given in Theorem 3.17 for the characteristic arcs emanating from the positions (48). A rigorous proof of this statement remains an open problem. The next section will contain some justification based on the results of numerical simulations for a sufficiently large finite horizon  $T$ .

*Conjecture 3.19* Under Assumptions 2.1–2.4, 3.3, 3.5, 3.8, 3.10, 3.12–3.15, the saddle state-feedback control map for the differential game (13)–(15) in case  $T = +\infty$  takes the form (61).

In the related characteristic portrait (see Fig. 3a), one can see the attractor  $(M^{**}, M^{**})$ , which is reached in finite time either through the diagonal  $M_1 = M_2$  (invariant in forward time), or from the domains  $G_{13}, G_{24}$ , or through one of the turnpike curves  $\Sigma_1$ – $\Sigma_4$ . After entering the attractor, the forward-time characteristics stay there indefinitely.

#### 4 Finite-difference approximation

We have used the software ROC-HJ [54] in order to approximate the viscosity solution of the problem (19) (*i. e.*, the value function  $V_{\text{VREK}} = V_{\text{s-f}} = V$  of the differential game (13)–(15) in nonanticipative or state-feedback strategies) for the time horizon  $T = 60$ , functions (5)–(7), and parameter values (10) by the method of finite differences [48, 50–52]. For numerical purposes, it is convenient to rewrite (19) in reverse time  $\tau \stackrel{\text{def}}{=} T - t$  as

$$\begin{cases} \frac{\partial V(T - \tau, M_1, M_2)}{\partial \tau} + \max_{u_1 \in [0,1]} \min_{u_2 \in [0,1]} \left( -H \left( T - \tau, M_1, M_2, u_1, u_2, \frac{\partial V(T - \tau, M_1, M_2)}{\partial M_1}, \frac{\partial V(T - \tau, M_1, M_2)}{\partial M_2} \right) \right) = 0, \\ V(T - \tau, M_1, M_2)|_{\tau=0} = 0, \\ \tau \in [0, T], \quad (M_1, M_2) \in G, \end{cases} \quad (62)$$

and then to rewrite (62) in the new state variables

$$m_i \stackrel{\text{def}}{=} M_i \cdot 10^{-4}, \quad i = 1, 2$$

(such changes of the time and state variables will lead to equivalent approximation results). Let us take  $\bar{M}_1 = \bar{M}_2 = \bar{M} = 3.5 \cdot 10^4$ ,  $\bar{m} \stackrel{\text{def}}{=} \bar{M} \cdot 10^{-4} = 3.5$  and discretize the computational region

$$\{(m_1, m_2, \tau) : 0 \leq m_1 \leq \bar{m}, 0 \leq m_2 \leq \bar{m}, 0 \leq \tau \leq T\}$$

by the spatial step  $\Delta m_1 = \Delta m_2 = \Delta m = 2 \cdot 10^{-3}$  and time step  $\Delta \tau = 5 \cdot 10^{-3}$ . For achieving faster practical convergence, it is reasonable to apply the second-order ENO scheme (for approximating the partial derivatives with respect to the state variables) coupled with the second-order Runge–Kutta time discretization scheme [51, 54]. In fact, we have also tested the classical first-order monotone Lax–Friedrichs scheme [50, 51, 54] (which ensures a theoretical convergence property and an error estimate), and it has given similar results, but with slower actual convergence.

After obtaining the value function  $V$ , an efficient practical way of constructing the saddle state-feedback control strategies outside the switching sets is to use the representations (21) with numerical approximations of the partial derivatives  $\partial V / \partial M_i$ ,  $i = 1, 2$ , although this is not completely rigorous if the gradient of  $V$  has discontinuities. Note that, due to the general properties of value functions for zero-sum closed-loop differential games [52, 55] and boundedness of the strongly invariant domain  $G$ , the value function  $V$  for our problem is Lipschitz continuous in  $[0, T] \times G$ , and, by Rademacher’s theorem, it is differentiable almost everywhere in  $(0, T) \times G$  (except possibly a subset of Lebesgue measure zero). In order to compute the values of the partial derivatives  $\partial V / \partial M_i$ ,  $i = 1, 2$ , we have used the standard second-order symmetrized approximation [56, §5.7].

Figs. 4,5 illustrate the reductions of the approximate value function and corresponding saddle state-feedback control strategies to the coordinate plane

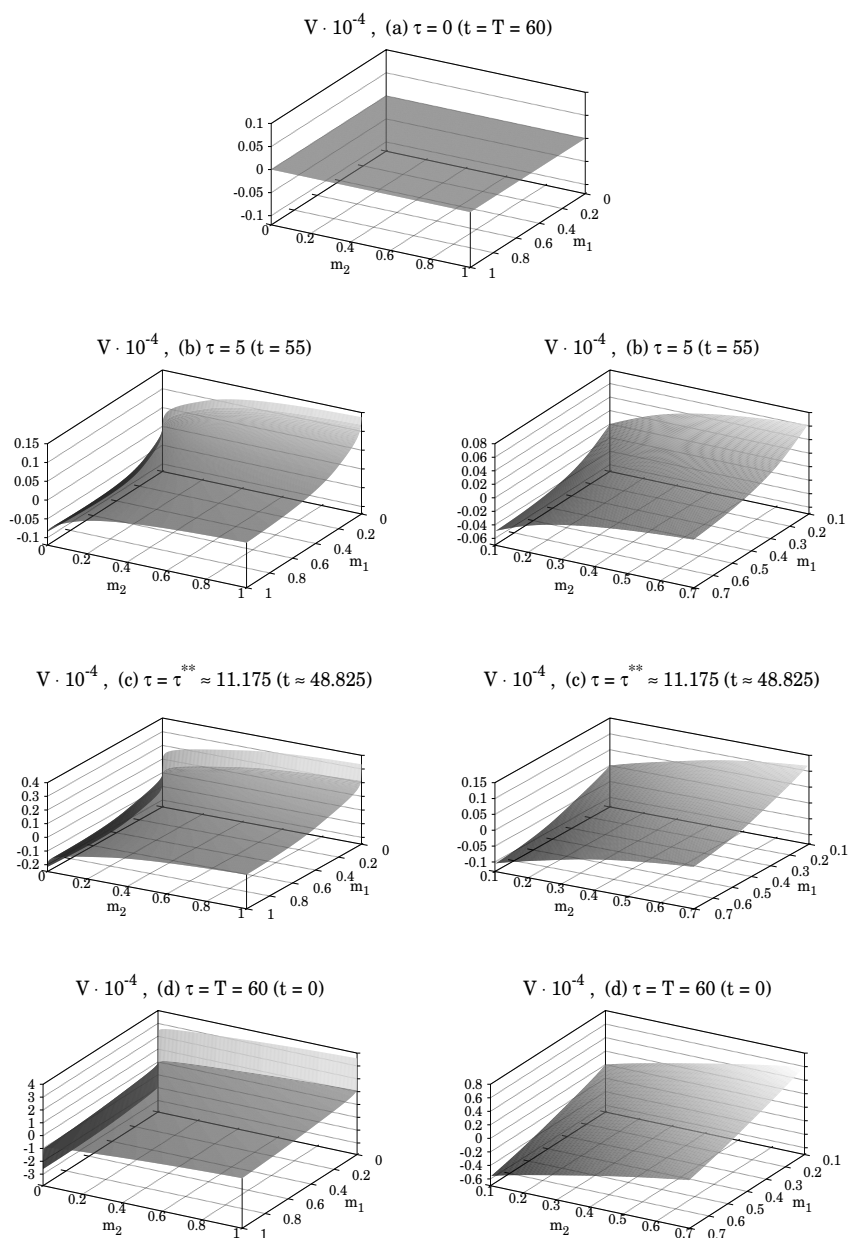


**Fig. 4** The finite-difference approximation of the value function  $V$  of the differential game (13)–(15) (in the nonanticipative or state-feedback sense) for the time horizon  $T = 60$ , functions (5)–(7), and parameter values (10). The subfigures illustrate the reductions to the domains  $(0, 1)^2$  and  $(0.1, 0.7)^2$  on the coordinate plane  $(m_1, m_2)$  for the time instants (a)  $\tau = 0$  ( $t = T = 60$ ), (b)  $\tau = 5$  ( $t = T - 5 = 55$ ), (c)  $\tau = \tau^{**} \approx 11.175$  ( $t = T - \tau^{**} \approx 48.825$ ), (d)  $\tau = T = 60$  ( $t = 0$ ). In order to see the graphs clearer, we do not fix the same scale for the vertical axes in the subfigures.

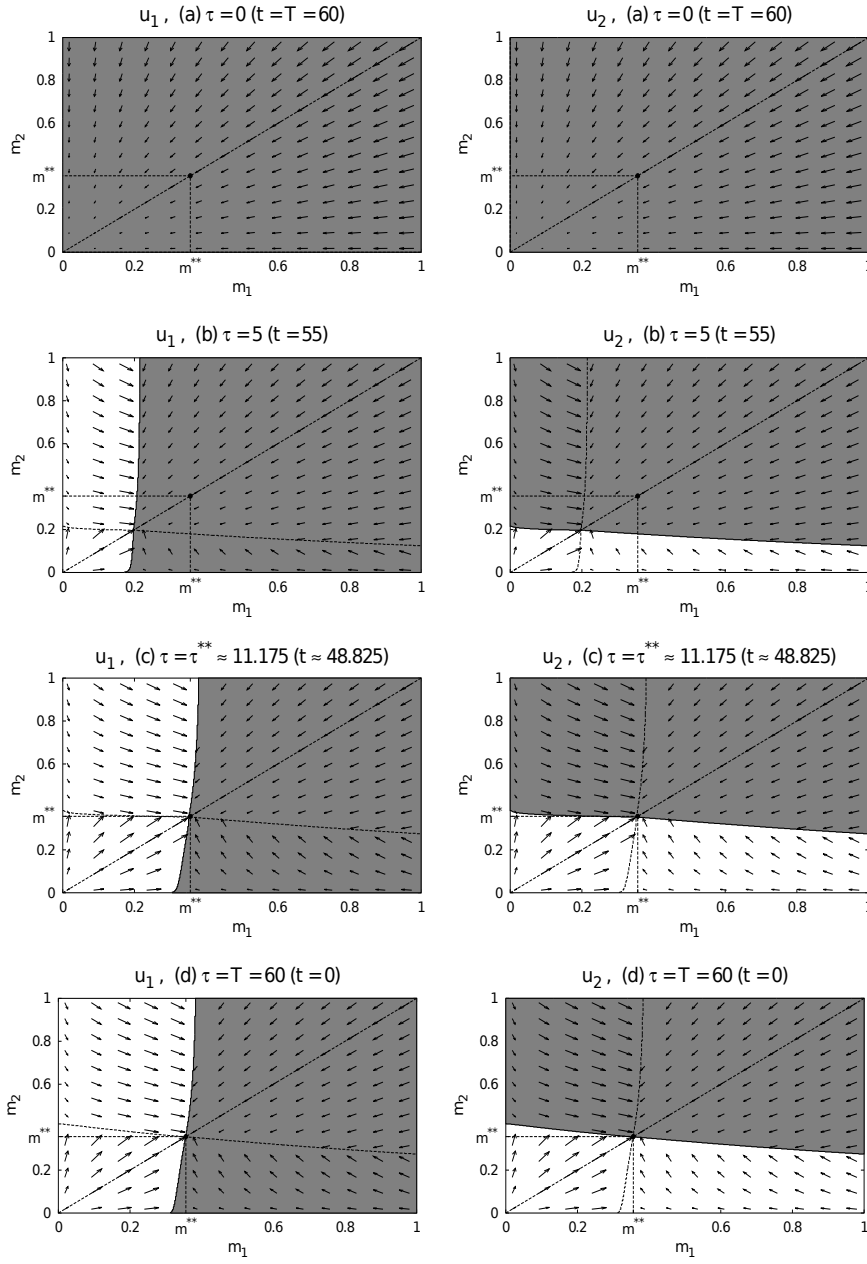


**Fig. 5** The finite-difference approximations of the saddle state-feedback control strategies in the differential game (13)–(15) for the time horizon  $T = 60$ , functions (5)–(7), and parameter values (10). The subfigures illustrate the reductions to the domain  $(0, 1)^2$  on the coordinate plane  $(m_1, m_2)$  for the time instants (a)  $\tau = 0$  ( $t = T = 60$ ), (b)  $\tau = 5$  ( $t = T - 5 = 55$ ), (c)  $\tau = \tau^{**} \approx 11.175$  ( $t = T - \tau^{**} \approx 48.825$ ), (d)  $\tau = T = 60$  ( $t = 0$ ). White and gray colors indicate regions of the control values 0 and 1, respectively. The fields of the related forward-time velocities are also shown.

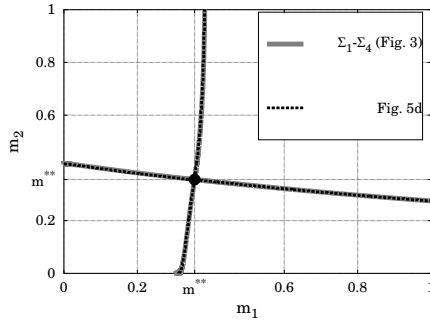


**Fig. 6** Comparison of the curves  $\Sigma_1$ – $\Sigma_4$  from Fig. 3 with the four approximate switching curves from Fig. 5d.

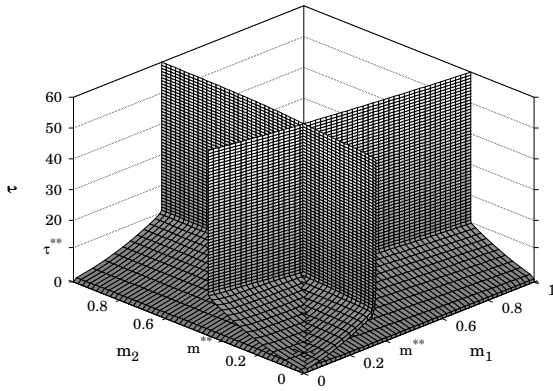


**Fig. 7** The four approximate switching surfaces in the coordinate space  $(m_1, m_2, \tau)$  for the closed-loop differential game (13)–(15) with the time horizon  $T = 60$ , functions (5)–(7), and parameter values (10).

$(m_1, m_2)$  for different time instants. As in Fig. 3, the portraits are depicted on relevant subregions of the strongly invariant domain  $G$ . Fig. 5 also shows the fields of the related forward-time velocities.

The reductions of the value function in Fig. 4 seem to be continuously differentiable. Moreover, they vanish on the diagonal  $m_1 = m_2$  (invariant for the forward-time characteristics), which leads to the conjecture that the two cohorts should have equal saddle state-feedback control strategies there. This also conforms with Fig. 3. Besides, if  $M_1^0 = M_2^0$ , then one can expect equality of the components in the resulting open-loop control pairs that arise from the definitions of nonanticipative strategies of the cohorts.

Fig. 5 indicates the appearance and time evolution of four approximate switching curves. For  $\tau \geq \tau^{**}$ , they intersect nearly at the point  $(m^{**}, m^{**})$ , where  $m^{**} \stackrel{\text{def}}{=} M^{**} \cdot 10^{-4}$ . With the further increase of  $\tau$ , the related feed-

back control portrait approaches the stationary form (61), as follows from the comparison in Fig. 6. The four resulting switching surfaces in the coordinate space  $(m_1, m_2, \tau)$  are illustrated in Fig. 7.

Thus, the obtained numerical simulation results can indeed serve as a practical justification for Conjecture 3.19.

From Fig. 5d, we conclude that, in the considered domain of initial states, the value  $V(0, M_1^0, M_2^0)$  of our zero-sum closed-loop differential game is negative for  $M_1^0 > M_2^0$ , zero for  $M_1^0 = M_2^0$ , and positive for  $M_1^0 < M_2^0$ . One can expect this to hold also in the infinite-horizon case (in particular, Conjecture 3.19 yields vanishing of the game value on the diagonal  $M_1^0 = M_2^0$ ). Then, in compliance with the definition of uninvadability given in Subsection 2.2, the obtained saddle state-feedback strategy of cohort 1 is uninvadable if  $M_1^0 \geq M_2^0$ . Similarly, the obtained saddle state-feedback strategy of cohort 2 is uninvadable if  $M_1^0 \leq M_2^0$ .

## 5 Some asymptotic properties in case of a large total lesion density

In [15, Section 6], it was shown that, for the optimal control problem (11),(12) under some reasonable conditions, the function

$$X^*(n) \stackrel{\text{def}}{=} n \cdot M^*(n)$$

(describing how the total mycelial size in the singular control regime depends on lesion density) should be strictly increasing, bounded, and therefore saturating on  $[0, +\infty)$ . This was natural from the biological point of view due to the presence of the competition term  $\nu(nM)$  in the model.

For the differential game (13)–(15), the function

$$X^{**}(n) \stackrel{\text{def}}{=} n \cdot M^{**}(n) \tag{63}$$

describes the dependence of the total mycelial (infection) size at the steady state  $(M^{**}, M^{**})$  on the total lesion density  $n \stackrel{\text{def}}{=} n_1 + n_2$ . Let us establish that (63) also saturates on  $[0, +\infty)$  under certain conditions including Assumptions 2.5, 2.6.

Assumption 2.5 yields that the inequality (38) holds for all  $M > 0$  and  $n \geq 0$ . Then, by using the item 6 of Assumption 2.4, we conclude that, for any  $n \geq 0$ , the number  $M^{**}(n)$  can be defined as a unique positive root of the equation (34) regardless of the bounds for the strongly invariant domain (recall the proof of Theorem 3.1).

**Theorem 5.1** *Let Assumptions 2.1, 2.3, 2.6 hold. Also let Assumption 2.4 hold with the modifications mentioned in Assumption 2.5. Then the function (63) is strictly increasing, bounded, and therefore saturating on  $[0, +\infty)$ .*

*Proof* Denote

$$\zeta(n, x) \stackrel{\text{def}}{=} \nu(x) \rho' \left( \frac{x}{n} \right) - g' \left( \frac{x}{n} \right) - \mu \quad \forall n > 0 \quad \forall x > 0.$$

According to the equation (34), we have

$$\zeta(n, X^{**}(n)) = 0 \quad \forall n > 0. \quad (64)$$

Since  $X^{**}(0) = 0$  and  $X^{**}(n) > 0$  for all  $n > 0$ , then it suffices to verify positivity of  $(X^{**})'(\cdot)$  and boundedness of  $X^{**}(\cdot)$  on  $(0, +\infty)$ .

For all  $n > 0$  and  $x > 0$ , we obtain

$$\begin{aligned} \frac{\partial \zeta(n, x)}{\partial n} &= -\frac{x}{n^2} \left( \nu(x) \rho''\left(\frac{x}{n}\right) - g''\left(\frac{x}{n}\right) \right) > 0, \\ \frac{\partial \zeta(n, x)}{\partial x} &= \nu'(x) \rho'\left(\frac{x}{n}\right) + \frac{1}{n} \left( \nu(x) \rho''\left(\frac{x}{n}\right) - g''\left(\frac{x}{n}\right) \right) < 0. \end{aligned} \quad (65)$$

For every  $n > 0$ , the pair  $(n, X^{**}(n))$  is the value at the point  $(n, 0)$  of the inverse to the mapping

$$(0, +\infty) \times (0, +\infty) \ni (n, x) \longrightarrow (n, \zeta(n, x)). \quad (66)$$

The Jacobian of (66) is nonzero for any  $n > 0$  and  $x > 0$  by virtue of (65). Then, by the classical inverse mapping theorem,  $X^{**}(\cdot)$  is continuously differentiable on  $(0, +\infty)$ , and

$$\frac{dX^{**}(n)}{dn} = -\frac{\frac{\partial \zeta(n, X^{**}(n))}{\partial n}}{\frac{\partial \zeta(n, X^{**}(n))}{\partial x}} > 0 \quad \forall n > 0.$$

If there exists a sequence  $\{n_l\}_{l=1}^{\infty}$  of positive numbers such that  $\lim_{l \rightarrow \infty} n_l = +\infty$  and  $\lim_{l \rightarrow \infty} X^{**}(n_l) = +\infty$ , then, due to Assumptions 2.5, 2.6, we get

$$\limsup_{l \rightarrow \infty} \zeta(n_l, X^{**}(n_l)) \leq -\mu < 0,$$

which contradicts with (64). Thus,  $X^{**}(\cdot)$  is bounded on  $(0, +\infty)$ .  $\square$

*Remark 5.2* Let Assumptions 2.1, 2.3, 2.6 hold. Also let Assumption 2.4 hold with the following modifications: in its items 1–5, the intervals are extended up to  $+\infty$ , and, in its item 7,  $\tilde{M} \in (0, \tilde{M}_{\min})$  is replaced with  $\tilde{M} > 0$ . Moreover, suppose that  $n_1 > 0$ ,  $n_2 > 0$ , and that  $\rho(M) = \alpha M$  and  $g(M) = \gamma M$  for all  $M \geq 0$ , where  $\alpha, \gamma$  are positive constants (all these conditions hold in Example 2.9, while Theorem 5.1 adopts Assumption 2.5 including negativity of  $\rho''(\cdot)$  on  $(0, +\infty)$ ). Then (64) and (65) yield that  $dX^{**}(n)/dn = 0$  for all  $n > 0$ , i. e., the total steady-state mycelial size  $X^{**}(n)$  does not depend on the total lesion density  $n > 0$ . By applying similar arguments to the equation (36) for the single-cohort optimal control problem, one can derive that  $X^*(n)$  does not depend on  $n > 0$  under the additional condition that  $x\nu''(x) + 2\nu'(x) \neq 0$  for all  $x > 0$  (which also holds in Example 2.9). From the biological point of view, these conclusions seem to be less reasonable than the saturating growth behavior mentioned in Theorem 5.1 and in [15, Section 6]. Indeed, the total infection size is expected to increase with the increase of the total lesion density, at least when the latter is not very large.  $\square$

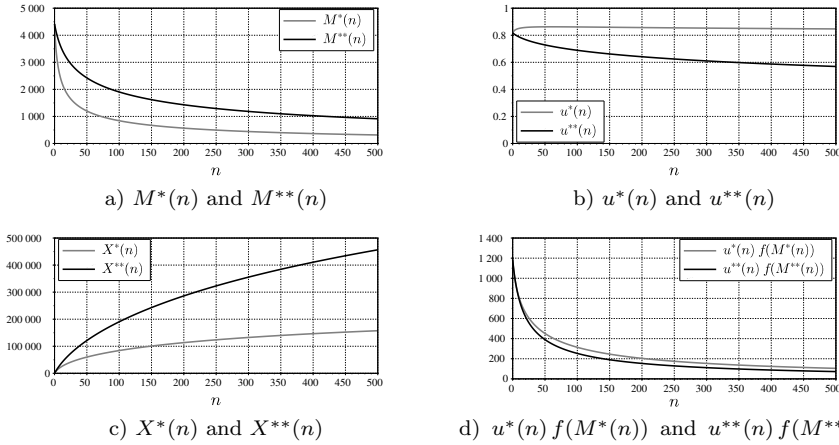


**Fig. 8** The graphs of the functions (a)  $M^{**}(n)$ , (b)  $u^{**}(n)$ , (c)  $X^{**}(n)$ , (d)  $u^{**}(n)f(M^{**}(n))$  in case of the representations (5)–(7) and values of all the model parameters except  $n_1, n_2, n$  as in (10). The graphs of the functions (a)  $M^*(n)$ , (b)  $u^*(n)$ , (c)  $X^*(n)$ , (d)  $u^*(n)f(M^*(n))$  are also shown for comparison.

Now let us adopt the representations (5)–(7) with  $n \geq 0$  and positive constants  $\alpha, k, \beta, \gamma$  satisfying the inequality (8). Then all the conditions of Theorem 5.1 hold. For numerical simulations, let us also choose the values of all the model parameters except  $n_1, n_2, n$  as in (10).

Fig. 8 illustrates the graphs of the functions  $M^{**}(n)$ ,  $u^{**}(n)$ ,  $X^{**}(n)$  and  $u^{**}(n)f(M^{**}(n))$ . The graphs of the functions  $M^*(n)$ ,  $u^*(n)$ ,  $X^*(n)$  and  $u^*(n)f(M^*(n))$  are also shown for comparison. For positive  $n$  in the indicated argument range, the following properties can be seen:

- $M^*(n) < M^{**}(n)$  (in conformity with (37));
- $u^*(n) > u^{**}(n)$ , *i. e.*, maintaining the singular control regime for the uninventable strategies requires lower relative investment in spore production and, consequently, greater relative investment in mycelial growth, compared to the optimal control case;
- $u^*(n)f(M^*(n)) > u^{**}(n)f(M^{**}(n))$ , *i. e.*, the steady-state spore production rate for the uninventable strategies is smaller than that in the optimal control case;
- as  $n$  increases, the functions  $M^*(n)$ ,  $M^{**}(n)$ ,  $u^{**}(n)$ ,  $u^*(n)f(M^*(n))$  and  $u^{**}(n)f(M^{**}(n))$  decrease, while  $u^*(n)$  stays approximately constant;
- $X^*(n)$  and  $X^{**}(n)$  grow and saturate (in agreement with [15, Section 6] and Theorem 5.1).

Finally, let us fix  $M_1^0 = M_2^0 = 1$  (which means that a mycelium appears from one spore at the beginning of the infection period) and consider the corresponding latency times for the optimal control problem (11),(12) and differential game (13)–(15) in the infinite-horizon case  $T = +\infty$ . These are the times at which the related forward-time characteristics reach the states

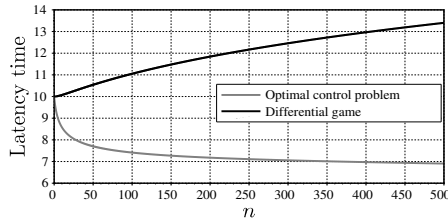


**Fig. 9** The dependence of the introduced latency times on  $n$  in case of the representations (5)–(7), values of all the model parameters except  $n_1, n_2, n$  as in (10), and initial state coordinates  $M_1^0 = M_2^0 = 1$ .

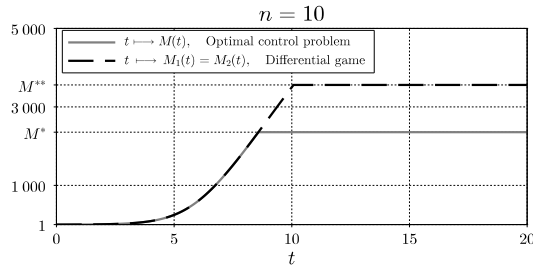


**Fig. 10** The trajectories  $t \mapsto M(t)$  (optimal control problem) and  $t \mapsto M_1(t) = M_2(t)$  (differential game) determining the introduced latency times in case of the representations (5)–(7), parameter values (10), and initial state coordinates  $M_1^0 = M_2^0 = 1$ .

$M = M^*$  and  $M_1 = M_2 = M^{**}$ , respectively (see Theorem A.13 in [Online Appendix A](#) and Conjecture 3.19). Let the observed range of positive  $n$  be such that  $M_1^0 = M_2^0 < M^*(n) < M^{**}(n)$  in it. From the biological point of view, the latency intervals therefore correspond to the time lags with no investment in spore production (zero-control regime).

Fig. 9 depicts the dependence of the introduced latency times on  $n$ . One can see that, starting already from sufficiently small positive  $n$ , the latency time function for the optimal control problem decreases, and the latency time function for the differential game increases. Hence, the influence of the competition term becomes strong enough to significantly slow the mycelial growth when approaching the average size  $M^{**}(n)$ , while approaching the lower size  $M^*(n)$  is not enough for increasing the related latency time with the increase of  $n$ . Besides, Fig. 9 indicates tending of the graphs to some horizontal asymptotes. The corresponding trajectories  $t \mapsto M(t)$  (optimal control problem) and  $t \mapsto M_1(t) = M_2(t)$  (differential game) in case of  $n$  specified by (10) are shown in Fig. 10. Thus, the game-theoretic competition makes  $M^{**}$  greater than  $M^*$  at the expense of a delayed onset of spore production.

## 6 Concluding remarks

This paper studied a game-theoretic extension of the continuous-time optimal resource allocation problem of [15]. We considered one-seasonal dynamics of two biotrophic fungal cohorts within a common host plant. From the perspective of Adaptive Dynamics, it was possible to interpret the cohorts as resident and mutant populations. The invasion functional took the form of the difference between the two marginal fitness criteria and represented the cost in the definition of the value of the differential game. The presence of a specific competition term in both equations and marginal fitnesses did not allow us to apply the two-step approach of [9–11] relying on Optimal Control Theory. Therefore, the general game-theoretic formulation of [11, §4.1] with the related concept of uninvadable strategy had to be used. From the mathematical point of view, it was reasonable to consider the class of state-feedback control strategies. The corresponding Cauchy problem for the HJI equation was investigated first analytically by the method of characteristics and then numerically by a finite-difference approximation scheme. The obtained analytical and numerical results turned out to be in good agreement with each other.

The approximated saddle state-feedback strategy of cohort 1 appeared to be uninvadable for  $M_1^0 \geq M_2^0$ , while the related strategy of cohort 2 became uninvadable for  $M_1^0 \leq M_2^0$  (recall the discussion in the end of Section 4).

The curves  $\Sigma_1$ – $\Sigma_4$  intersecting at the point  $(M_1, M_2) = (M^{**}, M^{**})$  played a crucial role in the analysis of the characteristics of the HJI equation (see Fig. 3). In such a reasonable abstraction as the infinite-horizon case, these were the only switching curves of the saddle state-feedback strategies of the cohorts (according to Conjecture 3.19). The corresponding control law (61) made the forward-time characteristics enter their attractor  $(M_1, M_2) = (M^{**}, M^{**})$  (either through the diagonal  $M_1 = M_2$ , or from the domains  $G_{13}, G_{24}$ , or through the intermediate turnpike regimes on  $\Sigma_1$ – $\Sigma_4$ ) and stay there indefinitely. In the finite-horizon case, additional switching surfaces in the space of the state and time variables appeared, but, for sufficiently large reverse time instants, the synthesis portrait became almost stationary and very close to the one specified by (61) (the related finite-difference approximation results served as a practical justification for Conjecture 3.19). It was also verified that, compared to the singular control regime  $M = M^*$ ,  $u = u^*$  in the single-cohort optimization problem of [15], maintaining the regime  $M_1 = M_2 = M^{**}$ ,  $u_1 = u_2 = u^{**}$  for the uninvadable strategies in the zero-sum differential game would require greater resources (recall Theorem 3.1 and Remark 3.2).

Furthermore, noteworthy asymptotic properties were established. In particular, it was shown that the total infection size at the steady state  $(M^{**}, M^{**})$  should saturate for large total lesion densities. This was reasonable from the biological point of view, because host resources were limited and, when increasing the lesion density, the infections could not infinitely grow. Some numerical experiments were conducted for such a significant pathogen trait as latency time. It also saturated for large total lesion densities, and, in the game-theoretic case, it was greater than in the optimal control case (the game-theoretic competi-

tion made  $M^{**}$  greater than  $M^*$  at the expense of a delayed onset of spore production).

Finally, let us discuss possible future developments of this work. First, the formalism of [23] may help to rigorously prove Conjecture 3.19. Next, long-seasonal dynamics and related evolutionary equilibria of competing biotrophic fungal cohorts are worth investigating. Then specific discrete rules can be adopted in order to model the transition from one season to another [30, 57]. Moreover, note that, within the framework of Adaptive Dynamics, ESS-es can be defined as such equilibria of an appropriately formulated canonical equation (whose type depends on the class of considered traits) that maximize the invasion fitness in the corresponding resident environment [3, 8–10]. It is important to study not only these equilibria themselves but also whether they indeed represent evolutionary attractors or not, and how they can be approached through evolution. The recent methodology of [8–10] for treating function-valued traits cannot be directly applied to our model (mainly because of the competition term). Hence, it is important to extend existing theoretical frameworks for describing evolutionary dynamics of infinite-dimensional traits. Besides, as was already noted in Remark 2.10, it is relevant to build new consumer-resource type models that combine the approaches proposed in this work and in the paper [38]. Another promising area is designing canopy-level numerical modeling frameworks, *e. g.*, by extending the one tested in [38].

## Electronic supplementary material

**Online Appendix A: Single-cohort optimal control problem**  
(PDF)

**Online Appendix B: Accompanying considerations for the characteristics in the zero-sum two-cohort differential game**  
(PDF)

## Acknowledgements

The authors acknowledge the support of the French Agence Nationale de la Recherche 664 (ANR) under grant ANR-13-BSV7-0011 (project FunFit).

## References

1. Vincent, T. L. and Brown, J. S. *Evolutionary Game Theory, Natural Selection, and Darwinian Dynamics*. Cambridge University Press: Cambridge, 2005.
2. Geritz, S. A. H., Kisdi, É., Meszéna, G., and Metz, J. A. J. Evolutionarily singular strategies and the adaptive growth and branching of the evolutionary tree. *Evol. Ecol.* 1998; **12**(1): 35–57.
3. Dercole, F. and Rinaldi, S. *Analysis of Evolutionary Processes: The Adaptive Dynamics Approach and Its Applications*. Princeton University Press: Princeton, 2008.

4. Maynard Smith, J. and Price, G.R. The logic of animal conflicts. *Nature* 1973; **246**: 15–18.
5. Maynard Smith, J. The theory of games and the evolution of animal conflicts. *J. Theor. Biol.* 1974; **47**: 209–221.
6. Eshel, I. and Motro, U. Kin selection and strong stability of mutual help. *Theor. Popul. Biol.* 1981; **19**: 420–433.
7. Nowak, M.A. An evolutionary stable strategy may be inaccessible. *J. Theor. Biol.* 1990; **142**: 237–241.
8. Dieckmann, U., Heino, M., and Parvinen, K. The adaptive dynamics of function-valued traits. *J. Theor. Biol.* 2006; **241**: 370–389.
9. Parvinen, K., Heino, M., and Dieckmann, U. Function-valued adaptive dynamics and optimal control theory. *J. Math. Biol.* 2013; **67**: 509–533.
10. Metz, J.A.J., Stankova, K., and Johansson, J. The canonical equation of adaptive dynamics for life histories: from fitness-returns to selection gradients and Pontryagin’s maximum principle. *J. Math. Biol.* 2016; **72**: 1125–1152.
11. Bernhard, P., Grognaard, F., Mailleret, L., and Akhmetzhanov, A. ESS for life-history traits of cooperating consumers facing cheating mutants. [Research Report] RR-7314, INRIA, 2010. URL: <https://hal.inria.fr/inria-00491489v2>
12. Bernhard, P. Evolutionary dynamics of the handicap principle: An example. *Dyn. Games Appl.* 2015; **5**: 214–227.
13. Shaiju, A. and Bernhard, P. Evolutionarily robust strategies: Two nontrivial examples and a theorem. In: Pourtallier, O., Gaitsgory, V., and Bernhard, P. (Eds.) *Advances in Dynamic Games and Their Applications, Annals of the International Society of Dynamic Games*, volume 10. Birkhäuser: Boston, 2009.
14. Pontryagin, L.S., Boltyansky, V.G., Gamkrelidze, R.V., and Mishchenko, E.F. *The Mathematical Theory of Optimal Processes*. Macmillan: New York, 1964.
15. Yegorov, I., Grognaard, F., Mailleret, L., and Halkett, F. Optimal resource allocation for biotrophic plant pathogens. *IFAC-PapersOnline* 2017; **50**(1): 3154–3159.
16. Deacon, J.W. *Modern Mycology*. Blackwell Scientific: Oxford, 1997.
17. Hahn, M. The rust fungi: cytology, physiology and molecular biology of infection. In: Kronstad, J.W. (Ed.), *Fungal Pathology*. Springer Science: Dordrecht, 2000.
18. Boyle, B., Hamelin, R.C., and Séguin, A. In vivo monitoring of obligate biotrophic pathogen growth by kinetic PCR. *Appl. Environ. Microbiol.* 2005; **71**(3): 1546–1552.
19. Bancal, M.O., Hansart, A., Sache, I., and Bancal, P. Modelling fungal sink competitiveness with grains for assimilates in wheat infected by a biotrophic pathogen. *Annals of Botany* 2012; **110**(1): 113–123.
20. Silvani, V.A., Bidondo, L.F., Bompadre, M.J., Colombo, R.P., Pérgola, M., Bompadre, A., Fracchia, S., and Godeas, A. Growth dynamics of geographically different arbuscular mycorrhizal fungal isolates belonging to the ‘Rhizophagus clade’ under monoxenic conditions. *Mycologia* 2014; **106**(5): 963–975.
21. Gilchrist, M.A., Sulsky, D.L., and Pringle, A. Identifying fitness and optimal life-history strategies for an asexual filamentous fungus. *Evolution* 2006; **60**: 970–979.
22. Yong, J. *Differential Games: A Concise Introduction*. World Scientific: Singapore, 2015.
23. Bernhard, P. Singular surfaces in differential games: An introduction. In: Hagedorn, P., Knobloch, H.W., and Olsder, G.J. (Eds.) *Differential Games and Applications*, volume 3 of the series *Lecture Notes in Control and Information Sciences*, pp. 1–33. Springer-Verlag: Berlin, 1977.
24. Bernhard, P. Differential games: Closed loop. In: Singh, M.G. (Ed.) *Systems & Control Encyclopedia: Theory, Technology, Applications*, pp. 1004–1009. Pergamon Press: Oxford, New York, 1987.
25. Bernhard, P. Differential games: Isaacs equation. In: Singh, M.G. (Ed.) *Systems & Control Encyclopedia: Theory, Technology, Applications*, pp. 1010–1016. Pergamon Press: Oxford, New York, 1987.
26. Bernhard, P. Pursuit-evasion games and zero-sum two-person differential games. *Encyclopedia of Systems and Control* 2014; 1–7. DOI: 10.1007/978-1-4471-5102-9\_270-1
27. Krasovskii, N.N. and Subbotin, A.I. *Positional Differential Games*. Nauka: Moscow, 1974. In Russian.
28. Subbotin, A.I. *Generalized Solutions of First-Order PDEs: The Dynamical Optimization Perspective*. Birkhauser: Boston, 1995.

29. Melikyan, A. A. *Generalized Characteristics of First Order PDEs: Application in Optimal Control and Differential Games*. Birkhauser: Boston, 1998.
30. Akhmetzhanov, A. R., Grognard, F., Mailleret, L., and Bernhard, P. Join forces or cheat: Evolutionary analysis of a consumer-resource system. In *Advances in Dynamic Games*, volume 12 of the series *Annals of the International Society of Dynamic Games*, pp. 73–95. Springer: New York, 2012.
31. Akhmetzhanov, A. R., Grognard, F., and Mailleret, L. Optimal life-history strategies in seasonal consumer-resource dynamics. *Evolution* 2011; **65**(11): 3113–3125.
32. Clarke, F. H., Ledyaev, Yu. S., Stern, R. J., and Wolenski, P. R. *Nonsmooth Analysis and Control Theory*. Springer-Verlag: New York, 1998.
33. Metz, J. A. J. Fitness. In: Jørgensen, S. E. and Fath, B. D. (Eds.) *Encyclopedia of Ecology*, pp. 1599–1612. Academic Press: Oxford, 2008.
34. Sasaki, A. and Iwasa, Y. Optimal-growth schedule of pathogens within a host: switching between lytic and latent cycles. *Theor. Popul. Biol.* 1991; **39**: 201–239.
35. Day, T. Parasite transmission modes and the evolution of virulence. *Evolution* 2001; **55**: 2389–2400.
36. Day, T. Virulence evolution and the timing of disease life-history events. *Trends Ecol. Evol.* 2003; **18**: 113–118.
37. Murray, J. D. *Mathematical Biology. I. An Introduction. Interdisciplinary Applied Mathematics*, volume 17. Springer-Verlag: Berlin, Heidelberg, 2002.
38. Précigout, P.-A., Claessen, D., and Robert, C. Crop fertilization impacts epidemics and optimal latent period of biotrophic fungal pathogens. *Phytopathology* 2017; **107**: 1256–1267.
39. Friedman, A. *Differential Games*. John Wiley & Sons: New York, 1971.
40. Schmitendorf, W. E. Differential games with open-loop saddle point conditions. *IEEE Trans. Automat. Contr.* 1970; **15**: 320–325.
41. Schmitendorf, W. E. Existence of optimal open-loop strategies for a class of differential games. *J. Optim. Theory Appl.* 1970; **5**: 363–375.
42. Schmitendorf, W. E. Differential games without pure strategy saddle-point solutions. *J. Optim. Theory Appl.* 1976; **18**: 81–92.
43. Parthasarathy, T. and Raghavan, T. E. S. Existence of saddle points and Nash equilibrium points for differential games. *SIAM J. Control* 1975; **13**(5): 977–980.
44. Ivanov, G. E. Saddle point for differential games with strongly convex-concave integrand. *Math. Notes* 1997; **62**(5): 607–622.
45. Varaiya, P. P. On the existence for solution to a differential game. *SIAM J. Control* 1967; **5**(1): 153–162.
46. Roxin, E. Axiomatic approach in differential games. *J. Optim. Theory Appl.* 1969; **3**(3): 153–163.
47. Elliott, R. J. and Kalton, N. J. The existence of value in differential games. *Mem. Am. Math. Soc.* 1972; **126**: 1–67.
48. Fleming, W. H. and Soner, H. M. *Controlled Markov Processes and Viscosity Solutions*. Springer-Verlag: New York, 2006.
49. Berkovitz, L. D. The existence of value and saddle point in games of fixed duration. *SIAM J. Control Optim.* 1985; **23**(2): 172–196.
50. Crandall, M. G. and Lions, P.-L. Two approximations of solutions of Hamilton–Jacobi equations. *Math. Comput.* 1984; **43**: 1–19.
51. Osher, S. and Shu, C.-W. High order essentially non-oscillatory schemes for Hamilton–Jacobi equations. *SIAM J. Numer. Anal.* 1991; **28**(4): 907–922.
52. Botkin, N. D., Hoffmann, K.-H., and Turova, V. L. Stable numerical schemes for solving Hamilton–Jacobi–Bellman–Isaacs equations. *SIAM J. Sci. Comput.* 2011; **33**(2): 992–1007.
53. Isaacs, R. *Differential Games*. Wiley: New York, 1965.
54. Bokanowski, O., Desilles, A., Zidani, H., and Zhao, J. User’s guide for the ROC-HJ solver. May 10, 2017. Version 2.3. URL: <https://uma.ensta-paristech.fr/soft/ROC-HJ>
55. Subbotin, A. I. and Chentsov, A. G. *Optimization of Guaranteed Result in Control Problems*. Nauka: Moscow, 1981. In Russian.
56. Press, W. H., Teukolsky, S. A., Vetterling, W. T., and Flannery, B. P. *Numerical Recipes: The Art of Scientific Computing*. Cambridge University Press: New York, 2007.
57. Mailleret, L. and Lemesle, V. A note on semi-discrete modelling in life sciences. *Philos. Trans. R. Soc. Lond. A* 2009; **367**: 4779–4799.